ON THE THEORETICAL ASPECTS OF MULTI-CARRIER SPREAD SPECTRUM SYSTEMS

BY

TSAN-FAI HO

A THESIS

Submitted in partial fulfillment of the requirements
for the degree of Master of Philosophy in the
Department of Information Engineering
The Chinese University of Hong Kong.

June 1996

香港中文大學
大學
圖書館系統
09 MAY 1997
UNIVERSITY
LIBRARY SYSTEM
THE CHINESE UNIVERSITY OF HONG KONG

Acknowledgments

I am pleased to express my heartfelt thanks to my advisor, Prof. Keh-Wei Wei for his in-depth guidance and supervision throughout the development of this thesis. Besides, he together with Prof. Tak-Shing Yum, Prof. Wai-Ho Yeung and Prof. Kwok-Wai Cheung also help me a lot in my future career planning.

A special acknowledgement is due to Dr. Branislav Popovič, whose assistance was invaluable at many critical points in the development of this material.

I am particular indebted to the reviewers of all my submissions and my colleagues who contribute directly or indirectly to my preparation in this thesis. They are Mr. Tat-Keung Chan, Mr. Chi-Wan Sung, Mr. Cheuk-Hung Lam, Mr. Hon-Hei Yau, Mr. Ji-Heng Yooh and Mr. Chi-Kit Yeung.

Last but not the least, I would like to express my great appreciation to my family and friends: June, Mabel, Connie, Eva, Mandy, Annie and Rebecca; for their kindliness encouragement and infallible support.

Abstract

Code division multiple access (CDMA) is a well known technique to cope with jamming and interference in various types of communication systems. In our study, we focus on the CDMA techniques incorporated with multiple carriers and analyze its performance (maximum number of users can be supported with a given *probability of error*). Study found that under the Gaussian Approximation (G.A.), Multi-Carrier (MC) CDMA has better error performance than the conventional DS-CDMA with random signature sequences.

We then study the spectral efficiency, the crest factor of the transmitted signals and the waveform synthesis in both time and frequency domain for MC-CDMA system. In time domain, MC-CDMA signals with low crest factor (*peak-to-average* ratio) are synthesized and its performance is then compared with those obtained in direct sequence (DS) CDMA using pseudo-random sequences. When using Golay complementary sequences as signature sequences in MC-CDMA, the crest factor is upper bounded by 6dB regardless of sequences' lengths, whereas the crest factors of the DS-CDMA pulses with pseudo-random sequences are dependent on the lengths of the sequences used and can grow without bound. Besides, bandwidth efficiency of the transmitted signals is of major concern in the mobile radio communications. It would be highly desirable if the transmitted signal has a steep roll-off at the band-edges of its power spectrum. A set of spectrally efficient complementary (SEC) sequences is found that can constitute MC-CDMA signals with both low crest factor (time-domain) and sharp spectral roll-off gradient (frequency-domain). SEC sequences are both synthesized over alphabet $\alpha_2 = \{-1, +1\}$ and $\alpha_4 = \{-j, -1, +j, +1\}$. Finally, methods of constructing SEC sequences are given and their applications to MC-CDMA are discussed.

Table of Contents

Chapter

List of Tables

List of Figures

Chapter 1

Introduction

1.1 Review on spread spectrum communications

Spread spectrum (SS) or *broadbanding* was defined as a means of communication using modulation to combine the information bearing with a specific signature (usually constructed from a *pseudo random* signature sequence, with the same signature used for data recovery [1]). The basic idea of spread spectrum is to conceal the transmitted signal from the unintended bodies. Methods are developed either to keep down the transmitted signal power or make the transmitted signal difficult to be recognized by others. One might even vary the frequency bands used or time-slots in order to achieve the goal of private communications. All the above strategies have a common characteristic that the resultant spectrum usage is far greater than the required bandwidth of the intended signal for transmission.

The advantages of spread spectrum communications include [2]: selective addressing; multiple access; low probability of intercept (LPI); high resolution ranging and anti-jamming (AJ), while it has the major drawback of inefficient bandwidth usage. There are various means by which the spectrum is spread [1], and we will discuss them in the following section.

1.2 The spread spectrum techniques

Under the definition of the above section, there are four classes of spread spectrum techniques [3]:

(i) Direct Sequence Systems;

(ii) Frequency Hopping Systems;

(iii) Time Hopping Systems;

(iv) Hybrid Systems.

The "Pulse-FM" or "chirp" system may also be classified as a type of spread spectrum technique [4], but it violates our definition of spread spectrum system by not using signature encoding. In fact, it is normally employed in radar applications by means of swept-frequency pulses.

1.2.1 Direct Sequence (DS) Systems

In general, this type of spread spectrum system uses a set of primitive polynomials and a pre-programmed N-state shift register for the generation of *pseudo random* or *pseudo-noise* (PN) signature sequences $\{c_n\}$ with period $2^N - 1$, the signature waveform $c_{DS}(t)$ is given by:

$$c_{DS}(t) = \sum_n c_n w_{T_c}(t - nT_c), \tag{1.1}$$

where $w_{T_c}(t)$ is the waveform shaping function with duration T_c, which is the chip period. Normally, the elements of the signature sequence are chosen to be either '+1' or '−1' (i.e. alphabet = $\{-1, +1\}$). The common modulation format used is BPSK or QPSK.

1.2.2 Frequency Hopping (FH) Systems

The idea of FH-SS systems is to adjust the carrier over a set of frequencies according to a specified *hopping pattern*, which is derived from the pseudo random signature sequence. The system with the carrier hopping rate faster (slower) than the information rate is

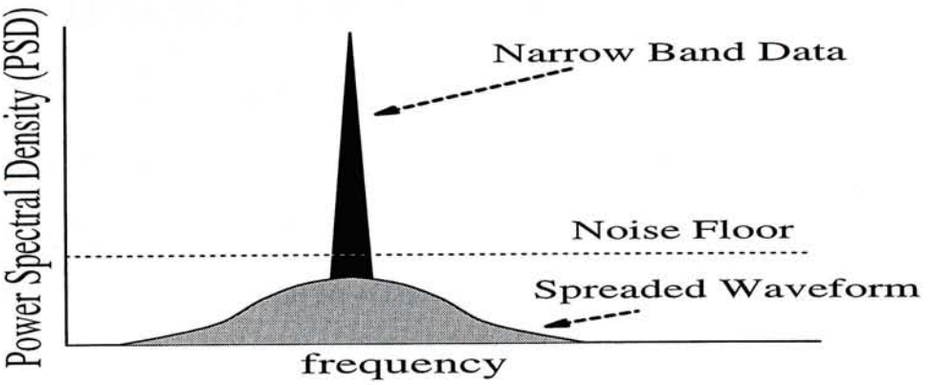

Figure 1.1: Frequency spectrum of DS-SS systems.

known as fast (slow) frequency hopping. The system can be implemented by using a frequency synthesizer and a PN sequence generator, while the signature waveform $c_{FH}(t)$ can be expressed as:

$$c_{FH}(t) = \sum_{n} \cos(2\pi f_n t + \phi_n) \cdot w_{T_h}(t - nT_h), \tag{1.2}$$

where f_n is the random frequency component, ϕ_n is the carrier offset or phase misalignment of the carrier derived from the frequency synthesizer, T_h is the duration of hopping with the pulse shaping function $w_{T_h}(t)$. It is noted that the signature sequences used may not necessarily to be binary as those in DS-SS systems and either noncoherent FSK or MSK is commonly incorporated with this system.

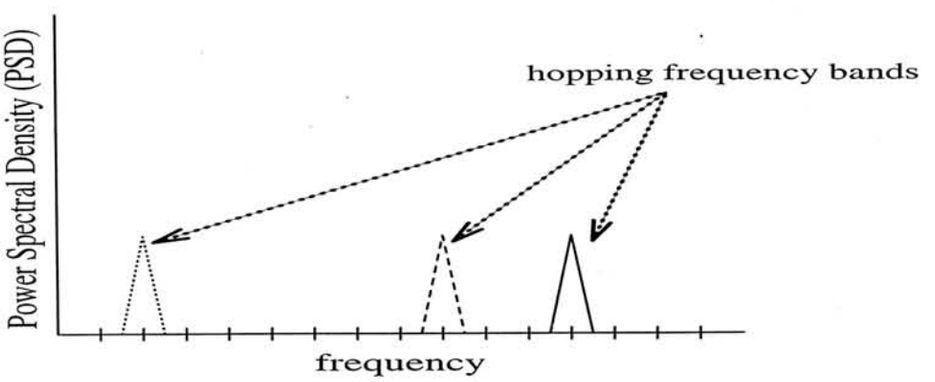

Figure 1.2: Frequency spectrum of TH-SS systems.

1.2.3 Time Hopping (TH) Systems

Unlike FH-SS systems, the TH-SS systems belong to a class of burst-mode transmission, which use a set of time-slots rather than a set of frequency bands for the spectrum spreading. In TH-SS systems, every symbol period is generally divided into M_T equally spaced sub-intervals, the transmitted signal is then hopped from one interval to another. The time hopping waveform of a typical TH-SS system with a given symbol period T_s is given by [3]:

$$c_{TH}(t) = \sum_n w\left(t - \left(n + \frac{a_n}{M_T}\right)T_s\right). \tag{1.3}$$

where $a_n \in \{0, 1, \ldots, M_T - 1\}$ is a pseudo random number determined from the $\log_2 M_T$ bits of the random signature sequence. This type of system favoured the pulse modulation, e.g. PAM.

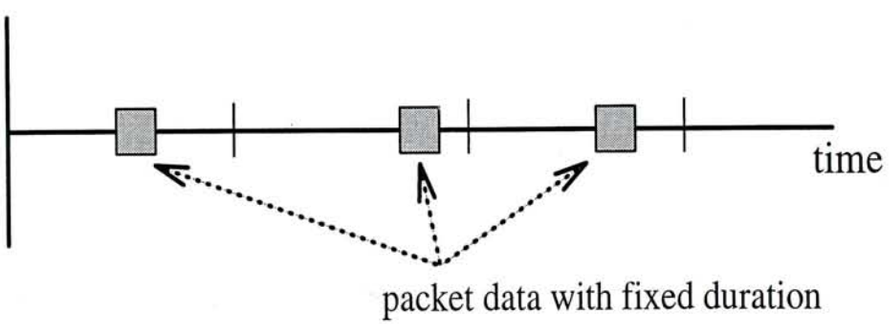

Figure 1.3: A snapshot in time domain in description of TH-SS systems.

1.2.4 Hybrid Systems

Each of the above techniques processes certain advantages and weaknesses. A spread spectrum system can be customized by combining two or more of the above techniques and to obtain the optimal desired performance with an increase in the system complexity. The common choice of the hybrid systems is TH/FH system, where it is mostly used in the situation with large number of sparsely populated users, each with different transmission power [5].

Given a SS system, the fundamental performance measures are known as *processing gain* and *jamming margin*, they are given as follows [2, 5]:

$$processing\ gain = G_p = \frac{BW_{RF}}{R_{inf}} \quad \text{and} . \tag{1.4}$$

$$jamming\ margin \approx G_p - \left(\frac{S}{N}\right)_{min}, \tag{1.5}$$

where BW_{RF} is the transmitted signal bandwidth in the passband and R_{inf} is the information rate at the baseband, while $(S/N)_{min}$ is the minimum tolerable signal-to-noise ratio at the input of the receiver.

1.3 Existing Applications of the spread spectrum systems

The concept of spectrum broadening dated back to the mid 40s, when R. H. Dicke and S. Darlington patented their works on a chirp pulse radar [3]. In the Second World War, spread spectrum was one of the useful tools in military communication systems (e.g. ARC-50 family of systems) and various types of patents emerged in the areas of range measurement and noise-radar. Moreover, there were applications available on private communications, such as X-System or Project X-61753 at Bell Labs providing the security of a one-time-pad crypto-system [3].

Nowadays, spread spectrum (SS) communication systems have been deployed in commercial areas. Nearly all the products related to SS is classified as Part 15 according to Federal Communication Commission (FCC). These products available include: wireless local area network, spread spectrum satellite (e.g. PANSAT by Space Systems Academic Group at the Naval Postgraduate School in Montreal [4]) and wireless code-division-multiple access (CDMA) personal communications system (e.g. QualComm CDMA, IS-95). Among all the available services, cellular CDMA seems to be the most popular one. Not only does it offer good service quality and network capacity, but it also maintains flexibility in the system design and operation [6].

1.4 Organization of the thesis

In this thesis, we study a new type of CDMA system which use multiple carriers in both the modulation and demodulation and it has been found that this MC-CDMA system outperforms the traditional DS-CDMA system.

In the following chapters, we would give a brief outline of the MC-CDMA system, following the performance analysis and comparison with those of the DS-CDMA under the issues of system capacity, waveforms design criteria, and spectral efficiency.

Chapter 2

The Concept of Duality

2.1 Multi-Carrier Systems – An Overview

Multi-Carrier modulation (MCM) is based on the manipulation of the transmitted signals in frequency-domain. The spectrum of the transmitted signal is equally divided into N subbands. A diagram of the frequency spectrum of a band-limited MCM is showed in Figure 2.1.

Unlike the conventional frequency-division multiplexing, different transmission rate can be allocated into different sub-bands in maximizing the overall performance using the *Shannongri-la* (water-filing) principle [7, 8]. The applications of MCM include: high speed modems, e.g. IMC, Telebit; High bit-rate Digital Subscriber Line (HDSL); and Digital Audio Broadcast (DAB) systems, e.g. Eureka 147 [7, 9]. One of the most striking examples of MCM is the Europe DAB project, which gains appeal by the capability

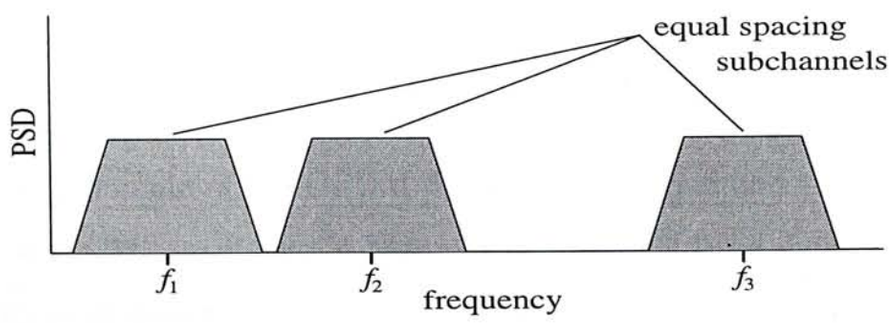

Figure 2.1: Frequency spectrum of MCM.

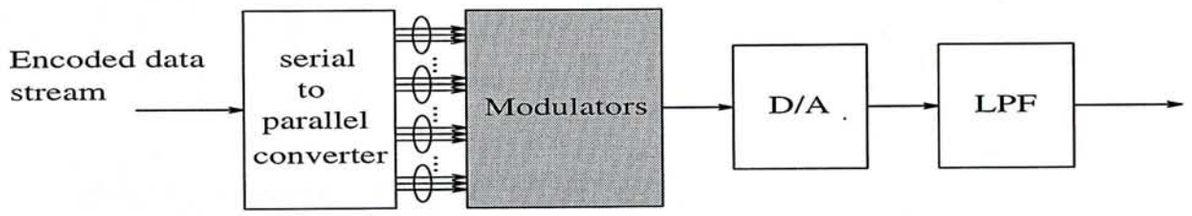

Figure 2.2: System model of a multi-carrier system.

of providing "multimedia" services. The transmission technique used is *Orthogonal Frequency Division Multiplexing* (OFDM).

2.2 Orthogonal Frequency Division Multiplexing

An example of multicarrier transmitter model for OFDM is shown in Figure 2.2, where the bank of modulators can be easily implemented by digital signal processing or simply *Fast Fourier Transform* (FFT). The spectrum of OFDM signal is similar to that shown in Figure 2.1, but with certain degree of overlapping among the subbands by proper selection of the symbol shapes and the frequency spacings. If the transmitted signal is a combination of sinusoids, the basic OFDM signal with N carriers can be described as:

$$s(t) = \sum_{n=1}^{N} b_n w(t - nT_s) e^{j(\omega_0 t + \psi)}, \tag{2.1}$$

where $w(t)$ is the impulse response of the transmission filter, T_s is the symbol interval, ω_0 is the carrier radian frequency, ψ is the carrier phase, and the sequence $\{b_n\}$ is the resultant of the Fast Fourier transform of the data $\{a_l\}$:

$$b_k = \frac{1}{N} \sum_{l=0}^{N-1} a_l \cdot e^{j2\pi kl/N}, k = 0, \ldots, N-1. \tag{2.2}$$

The frequency-domain of the OFDM (overlapping) signal and that of the single carrier modulation (SCM) are shown in Figure 2.3. The solid lines show the concatenation of the mutually orthogonal carriers in OFDM; and the dotted line represents the SCM. It can be observed that because of the non-rectangular spectrum of the symbol pulse

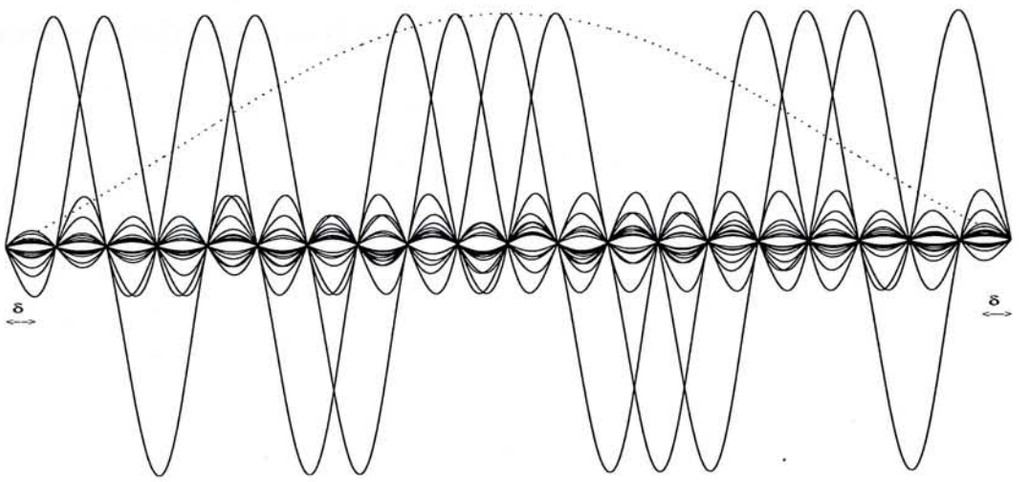

Figure 2.3: Symbol overlapping in OFDM.

shape, the spectral roll-off in the bandedges of OFDM signal is steeper than the single carrier transmission as N increases, while the orthogonal superposition of the subbands' spectra constitutes an approximately flat power spectrum with the following advantages [7]:

(i) Bandwidth efficient transmission,

(ii) High spectral efficiency,

(iii) Low sensitivity to burst errors and frequency-selective fading.

2.2.1 Bandwidth Efficiency

With M-ary signaling, $\log_2 M$ bits are transmitted over one symbol period. Let T be the symbol period of the information bearing and N be the total number of carriers used. The data rate is then given by $\frac{\log_2 M}{T}$. Because of the time-domain widening of the transmitted data, the frequency spacing between any two channels is $\frac{1}{NT}$. The actual bandwidth used on the other hand, is given by [10]:

$$f_N - f_1 + 2\delta, \tag{2.3}$$

where f_N and f_1 are the maximum and minimum carrier frequency respectively; and δ is generally expressed as $\frac{1+\gamma}{2NT}$ for $\gamma \in \{0, 1\}$. For orthogonal overlapping of the subcarriers, $f_N - f_1 = \frac{N-1}{NT}$.

The *bandwidth efficiency* is defined as:

$$\frac{\text{transmission rate}}{\text{total bandwidth used}}. \tag{2.4}$$

Thus, the bandwidth efficiency $\mathcal{B}_e$ of the OFDM signal with M-ary signaling is [10]:

$$\begin{aligned} \mathcal{B}_e &= \frac{\log_2 M}{\left(1-\frac{1}{N}\right)+2\delta T} \quad \text{(bits/s/Hz)}. \\ &= \frac{\log_2 M}{\left(1+\frac{\gamma}{N}\right)} \end{aligned} \tag{2.5}$$

We can therefore see that the bandwidth efficiency of OFDM signal approaches the ideal M-ary signaling if the number of carriers N is large and the roll-off factor γ is small (i.e. steeper roll-off near the bandedges of the overall frequency spectrum).

2.2.2 Spectral Efficiency

The spectral efficiency is defined as:

$$\frac{\text{in-band power}}{\text{total transmitted power}} \times 100\%, \tag{2.6}$$

The spectral efficiency of OFDM signals is shown in Figure 2.4. Thus, the orthogonal concatenation of the carriers leads to an advantage of less energy wastage than SCM ($N = 1$). It is therefore by this characteristic, make OFDM a promising scheme via bandwidth-limited environment.

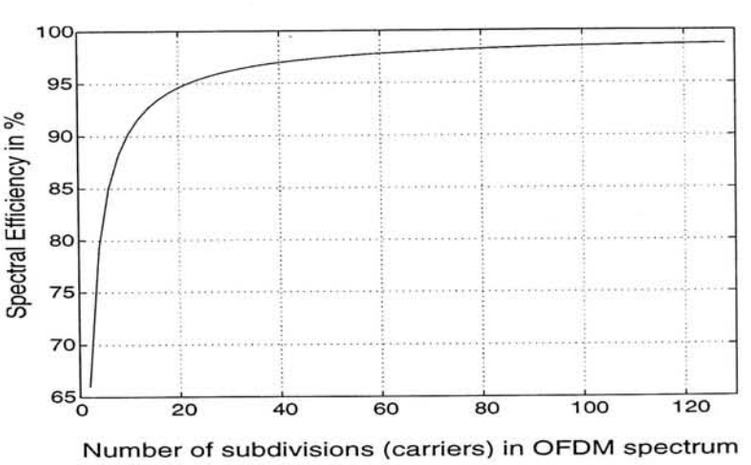

Figure 2.4: Spectral efficiency of OFDM signal.

In the above comparison, we assume that the impulse response of the transmission filter or simply *pulse shape* is rectangular symbol. It should be noted that the difference in spectral efficiency between SCM and OFDM is dependent on the pulse shape $w(t)$ used in (2.1).

2.2.3 Effects of fading

There is no doubt that the performance of a communication system can be seriously affected by the channel characteristics. As OFDM finds major application with the signaling in VHF or UHF bands, the time-varying statistics of the channels should be determined. The envelope of the fading consists of two components: long-term fading and short-term fading.

The long-term fading component is heavily dependent on the path loss in the terrain, which can be eliminated using proper planning and design of the cell site [10]. Moreover, the short-term fading of the microwave radio channel may be described by *multipath intensity profile* and *Doppler power spectrum.* The former is caused by the scattering of the transmitted signal with fixed objects (e.g. buildings); while the latter is resulted from the moving scatterers. It has been accepted that the short-term fading characteristics in mobile communications channel can be approximated to have a Rayleigh distributed fading envelope [10]. In the terrestrial environment, paths of the received signal are modelled using tapped delay lines (TPL) with each path associated with its propagation delay and attenuation factor. However, the paths may not exist in discrete format, thus the received signal and the lowpass equivalent impulse response $h_c(\tau, t)$ of the channel can be represented as [11]:

$$r(t) = \int_{-\infty}^{\infty} \alpha(\tau, t) s(t-\tau) d\tau \quad \text{and} \tag{2.7}$$

$$h_c(\tau, t) = \alpha(\tau, t) e^{-j2\pi f_c \tau} \tag{2.8}$$

where f_c is the RF carrier, $s(t)$ is the transmitted signal, $\alpha(\tau, t)$ is the attenuation of the signal with delay τ and at time t.

The multipath intensity profile describes the variation of the average power output against the time delay caused by the multipath environment, while it is essentially given

by [11]:

$$\phi_{h_c}(\tau) = \frac{1}{2}E\{|\alpha(\tau,t)|^2\}. \tag{2.9}$$

The *delay spread* or *multipath spread* T_m of the channel is defined as the range of τ such that $\phi_c(\tau)$ falls from its maximum value to zero. The reciprocal of the *delay spread* $1/T_m$ or simply the *coherence bandwidth* describes the condition for the transmitted signals as a whole that would share the same fading characteristics. For a transmitted signal with bandwidth $BW \gg 1/T_m$, part of the signal would fade independently, and the channel is considered as *frequency-selective*, and various means should be deployed for the equalization of the resulted intersymbol interference (ISI).

Besides, the time-varying nature of the channel constitutes an undesirable broadening of the signal spectrum (Doppler broadening). The Doppler power spectrum can be expressed as [12]:

$$S_{H_c}(\lambda) = \int_{-\infty}^{\infty} \phi_{H_c}(\Delta t)e^{-j2\pi\lambda\Delta t}d\Delta t \quad \text{and} \tag{2.10}$$

$$\phi_{H_c}(\Delta t) = \frac{1}{2}E\{H_c^*(f,t)H_c(f,t+\Delta t)\} \tag{2.11}$$

where $H_c(f,t)$ is the transfer function of the channel and λ is the Doppler frequency. The maximum frequency range for which $S_{H_c}(\lambda)$ exists is called the maximum Doppler spread, f_m; while the reciprocal of the maximum Doppler spread is the so-called "coherence time". If the symbol period of the transmitted signal is not much smaller than that of the *coherence time*, the fading of the channel is *time-selective*. Therefore, the condition for a *slowly time-varying frequency non-selective* (flat) fading channel is [12]:

$$T_m \ll T_s \ll \frac{1}{f_m}. \tag{2.12}$$

Not only does the parallel data transmission in OFDM make the channel apparently insensitive to the delay spread and the burst errors, the intersymbol interference (ISI) can also be randomized [10]. However, time variations of the channel may not be negligible and the effect of Doppler spread should be considered.

2.3 Applications of OFDM in multiple access

In a code-division multiple access application, several transmitters send signals to the same receiver, usually in the same frequency band and at the same time. In using OFDM for code-division multiple access, the main objective is to enable the receiver to distinguish the different messages sent by different receivers. This is the so-called "multiple access" problem. In contrast, the applications of OFDM to DAB and to Digital Subscriber loop, the main objective is to maximize the transmission rate in a broadcast communication system or a point-to-point communication system.

Several teams of authors have studied the application of the OFDM principle to code-division multiple access. These studies have minor differences in the exact system they use, yet they have acquired different names, such as:

(i) Spread-Time (ST) CDMA,

(ii) Multi-Carrier (MC) DS-CDMA,

(iii) OFDM-CDMA, or MC-CDMA.

2.3.1 ST-CDMA

ST-CDMA was proposed by Crespo et al. [13], which uses frequency-domain pulse shaper or *spectral encoder* to generate the transmitted signal. The method of signal generation requires extensive computation of the pulse shape before transmission in order to guarantee the output of the signals have the "noise-like" property.

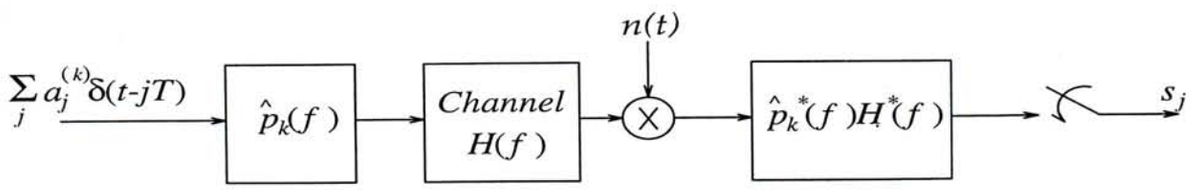

Figure 2.5: System model of ST-CDMA.

For a rectangular spectrum, the impulse response of the spectral encoder is designed as:

$$p(t) = \frac{\sin \pi f_c t}{\pi t} \sum_{n=-N/2}^{N/2-1} c_n e^{j2\pi f_c (n+\frac{1}{2})t}, \tag{2.13}$$

where $\{a_j\}$ and $\{c_n\}$ are the data and the signature sequences respectively, while f_c is the RF carrier frequency.

The basic advantage of this ST-CDMA is the flexibility in modifying the frequency spectrum during transmission (i.e. discontinued frequency bands) [13]. However, the spectral matching condition and the non time-limited pulse shape may cause it difficult in both implementation and performance evaluation.

2.3.2 MC-DS-CDMA

The Multi-Carrier DS-CDMA on the other hand, resembles the OFDM by using the serial-to-parallel converter to spread out every symbol in different subchannels before the modulation with the signature sequence waveform $c^{(k)}(t)$ as shown in Figure 2.6.

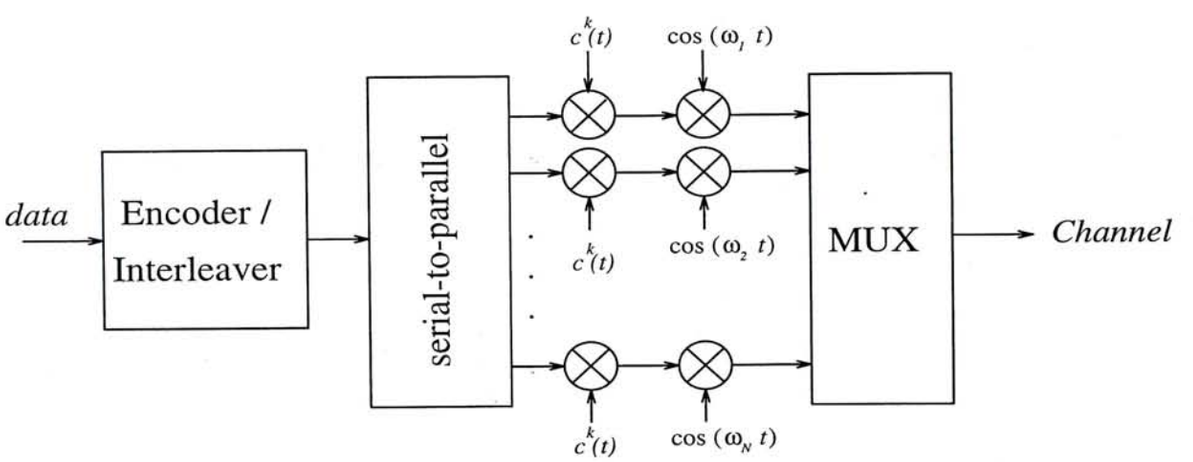

Figure 2.6: Transmitter of MC-DS-CDMA.

The system can be viewed as a parallel concatenation of N DS-CDMA systems using the same $c^{(k)}(t)$. In the frequency-domain, the signals from adjacent channels are orthogonally superimposed together to form the resultant transmitted frequency spectrum. However, the time-offset between any two subchannels are bounded by the

chip period T_c in order to maximize the performance [14] . Therefore, the intersymbol time interval may not be large enough for the receiver (e.g. RAKE) to resolve the multipath components.

2.3.3 OFDM-CDMA

In OFDM-CDMA system, the signal is generated by first modulated the signature sequence before passing through a serial-to-parallel converter. In this case, the chip period rather than the symbol period gets enlarged and the N $\sin x/x$ pulses in frequency domain are weighted by the signature sequences $\{c_n\}$. According to Fazel, the users are segregated into K groups before transmission [15]. For simplicity, we release the requirement of the grouping and set $K = 1$ in our system and the system model of one single user can be simplified as follows:

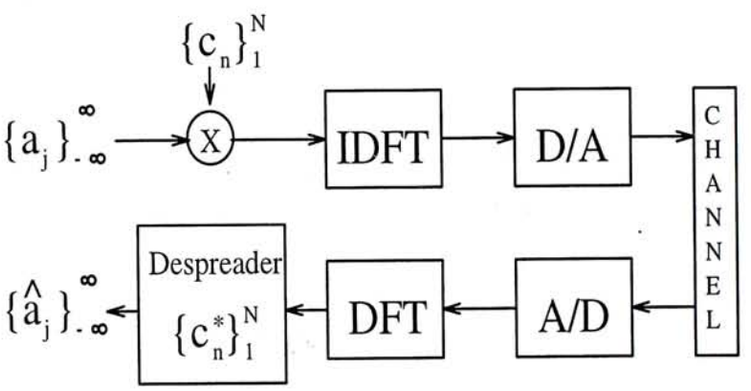

Figure 2.7: System model (baseband) of OFDM-CDMA.

The data sequence $\{a_j\}$ is assumed to be oscillating between -1 and $+1$, while $\{c_n\}$ is assumed to be a PN sequence at this instant. In the later chapter, we will release this constraint and show that using another type of sequence can actually improve the system performance. The DFT or IDFT block in Figure 2.7 is an efficient implementation of the blank of modulators and demodulators. The spreading of the chip period (S/P block) helps in combating the frequency-selective fading, and hence eliminate the inter-chip interference. It has been noted that there is a time-frequency interrelation (*duality*)

between the OFDM-CDMA and the conventional DS-CDMA system. This concept of duality would be covered in the next section.

2.4 Duality - Time-Frequency Interrelation

The time-frequency *duality* has long been studied. The application of the OFDM to multiple access is a particular "*dual* " of the conventional DS-CDMA system. In fact, all of the three systems discussed in the previous section have their respective "duality components" with the DS-CDMA. We will only focus on the OFDM-CDMA system as shown in Figure 2.7.

In OFDM-CDMA, the spreading is done in time-domain with the chips transmitted in parallel. The spectra of the N chips are the same (the Fourier transform of the symbol shape), and allocated to their corresponding carrier frequencies. The symbol shape in OFDM-CDMA can be designed using a time window rather than a filter. Finally, as the configuration of the OFDM is to mitigate the frequency-selective fading, a new type of channel should be used in the performance analysis which is the *time-selective* fading channel. The channel model and the performance analysis of the OFDM-CDMA would be detailed in chapter 3. In summary, the *duality components* are tabulated in Table 2.1. For simplicity, we will use the term MC-CDMA interchangeably with OFDM-CDMA in the following chapters.

Concept of duality		
System Component	**DS-CDMA**	**MC-CDMA**
Spreading	Frequency-domain	Time-domain
Transmission style	Chips in time series,	Chips in parallel
Pulse Shape Design	Filtering	Time-windowing
Channel Model	Frequency-selective fading	Time-selective fading

Table 2.1: Duality between DS-CDMA and OFDM-CDMA.

Chapter 3

Performance of Multi-Carrier CDMA System

In this chapter, the performance of multi-carrier (MC) CDMA system in the uplink (mobile-to-base) communication is analyzed. In our analysis follows, the concept of *duality* is deployed in defining the proper pulse shape and channel model as compared with those of the DS-CDMA.

3.1 System Model

In our system, every transmitter is characterized by the use of quadrature modulator (QM). The internal operation of quadrature modulator is shown in Figure 3.1. It will be shown later in the section that the combination of the quadrature components at the passband would actually reduce the bandwidth of the transmitted signal into half while providing necessary information for detection.

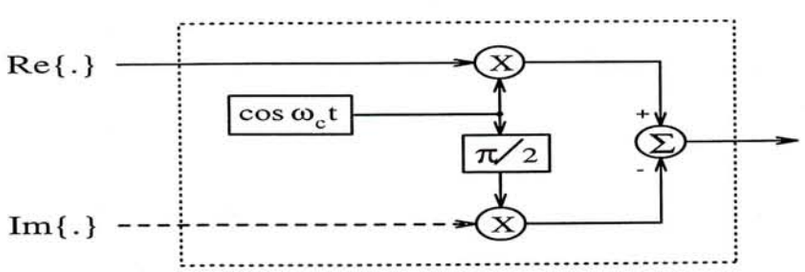

Figure 3.1: Quadrature modulator

The system model in the multiple access environment with M users is described in Figure 3.2.

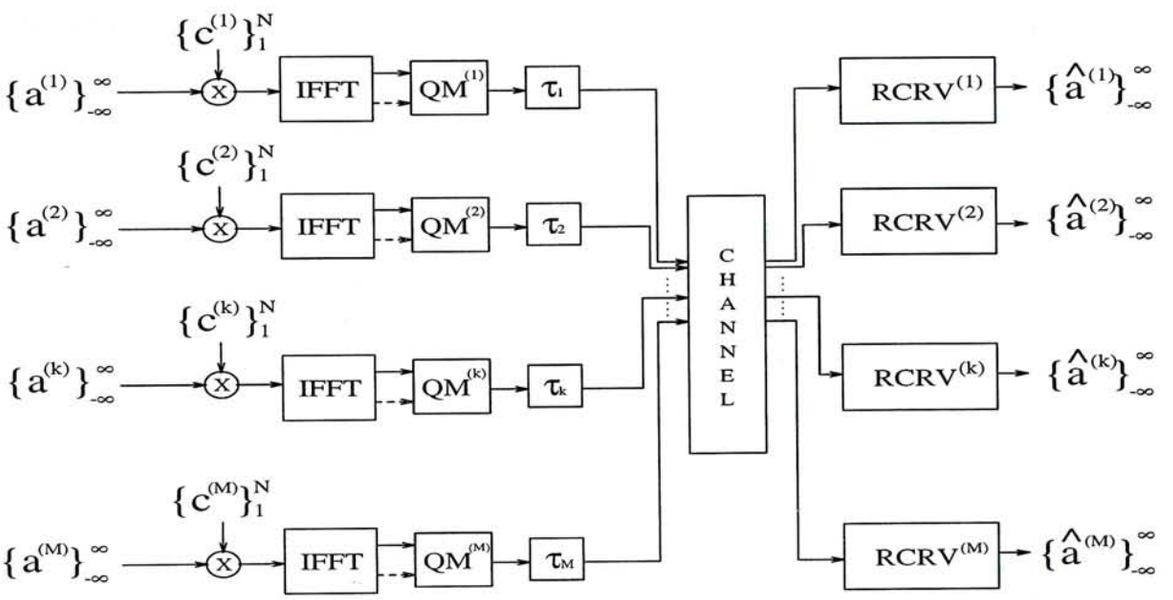

Figure 3.2: System model of MC-CDMA in multiple-access environment.

The transmitted signal of the kth user is in general shaped in the time domain by a window function $w(t)$ to minimize excessive out-of-band emissions. The quadrature sinusoidal carriers are then modulated by the real and imaginary part of the baseband signals generated from IFFT-style modulator bank (IFFT for short) respectively, while the former component at the jth symbol instant can be described as:

$$s_{\mathbf{I},j}^{(k)}(t) = \sqrt{\frac{2P}{N}} a_j^{(k)} \sum_{m=1}^{N} c_m^{(k)} \cos(\frac{2\pi mt}{T_s}) w(t - jT_s), \tag{3.1}$$

where $\{a_j^{(k)}\}$ is the bi-phase information sequence and $\{c_m^{(k)}\}$ is the spreading sequence over the alphabet $\{+1, -1\}$. It is assumed that the spreading gain N is large and equals the number of carriers present; while there is no intersymbol guard interval between adjacent symbols. The fundamental carrier frequency, f_0 equals the symbol rate $1/T_s$, and the transmitted signal power of every user is assumed to be the same (P say). Then, the jth transmitted symbol $s_j^{(k)}(t)$ of the kth user with modulator phase shift θ_k is:

$$s_{\mathbf{I},j}^{(k)}(t) \cos(2\pi f_c t + \theta_k) - s_{\mathbf{Q},j}^{(k)}(t) \sin(2\pi f_c t + \theta_k), \tag{3.2}$$

where f_c to $f_c + \frac{N}{T_s}$ is the desired spectrum in used and $s_{\mathbf{Q}}^{(k)}(t)$ equals (3.1) with the term $\cos(\frac{2\pi mt}{T_s})$ replaced by $\sin(\frac{2\pi mt}{T_s})$.

The addition of QM after the IFFT module in our system effectively restrict the frequency spectrum of the transmitted signal to be *single-sided.* The frequency spectrum of the baseband components $s_{\mathrm{I},j}^{(k)}(t)$ and $s_{\mathrm{Q},j}^{(k)}(t)$ are described pictorially as in Figure 3.3.

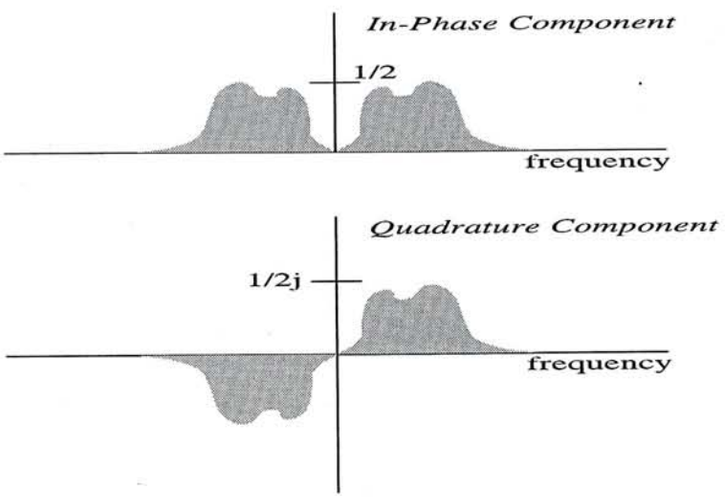

Figure 3.3: In-Phase and Quadrature components at baseband.

The combination of the two passband components would therefore reduce the usage of the bandwidth to half of the original bandwidth as shown in Figure 3.4. The effect of *sideband cancellation* is originated from the modulation format specified in the system model.

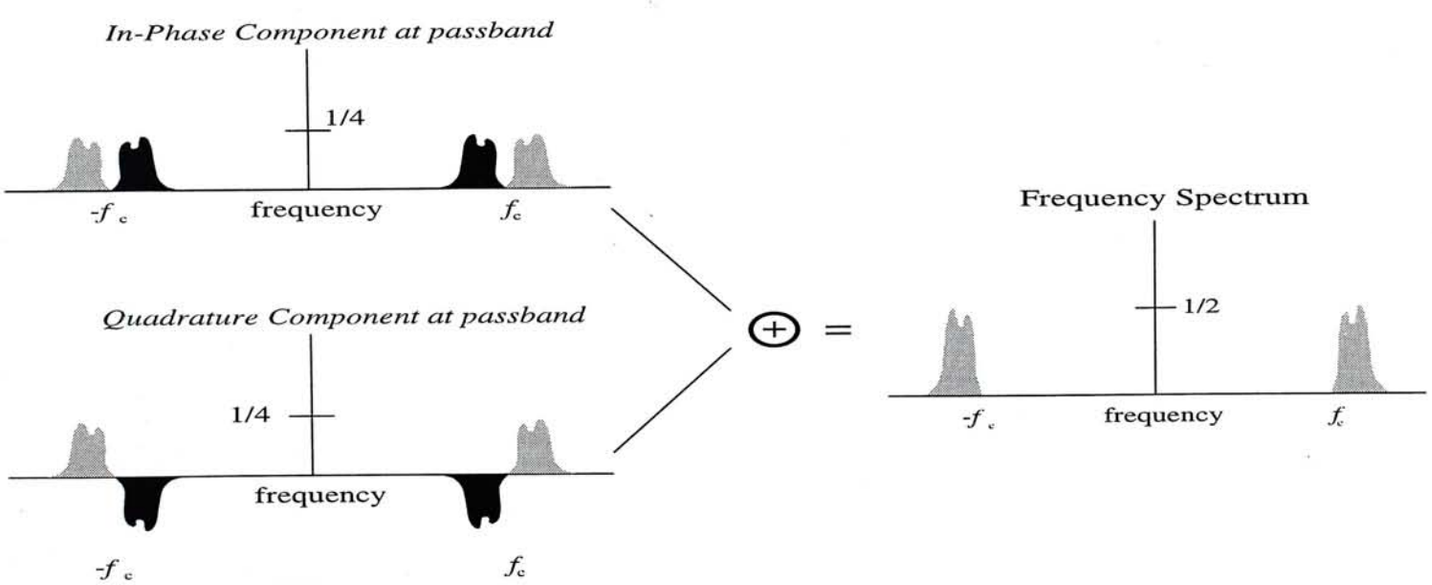

Figure 3.4: Generation of the transmitted signal at single-sided spectrum.

3.2 Performance Analysis

3.2.1 Gaussian Channel

For simplicity, we assume $w(t)$ in (3.1) equals $p_{T_s}(t)$, where

$$p_{T_s}(t) = \begin{cases} 1 & : \quad 0 \leq t \leq T_s \\ 0 & : \quad otherwise \end{cases} . \tag{3.3}$$

Let the intended receiver be $\text{RCVR}^{(1)}$ in Figure 3.2, where the transmitted data sequence $\{a_j^{(1)}\}$ is coherently detected and multipath fading is not present. The jth transmitted symbol at each receiver appears as

$$r_j(t) = \sum_{k=1}^{M} \left\{ s_{\mathbf{I},j}^{(k)}(t-\tau_k)\cos(2\pi f_c t + \varphi_k) - s_{\mathbf{Q},j}^{(k)}(t-\tau_k)\sin(2\pi f_c t + \varphi_k) \right\} + \mathcal{N}(t), \tag{3.4}$$

where $\mathcal{N}(t)$ is the white Gaussian noise and $\varphi_k = \theta_k - 2\pi f_c \tau_k$. The delay and the modified phase offset $\{\varphi_k\}$ of every transmitted signal are assumed to be uniformly distributed on the interval $[0, T_s]$ and $[0, 2\pi]$ respectively. It is further assumed that the parameters τ_1 and φ_1 equal zero. For simplicity, only the first symbol interval is considered and the demodulated signal at the intended receiver is

$$S^{(1)} + \sum_{k=2}^{M} I^{(1,k)} + \int_0^{T_s} \sum_{n=1}^{N} \mathcal{N}(t)\cos(2\pi n f_0 t)dt. \tag{3.5}$$

where $S^{(1)}$ is the useful output signal given by

$$S^{(1)} = a_0^{(1)} T_s \sqrt{\frac{NP}{2}}. \tag{3.6}$$

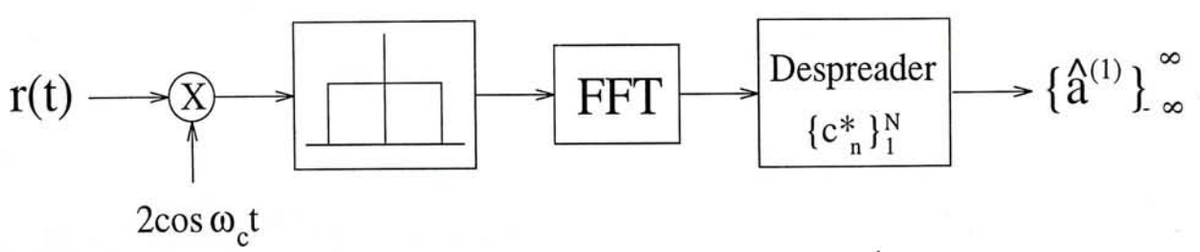

Figure 3.5: Receiver model of the intended user

The variance of the noise term in the (3.5) can be shown to be $NN_0T_s/4$ as follows.

$$\begin{aligned}
\sigma_{\mathcal{N}}^2 &= E[(\mathcal{N}-\mu_{\mathcal{N}})^2], \\
&= E\left[\int_{\lambda=0}^{T_s}\int_{t=0}^{T_s}\mathcal{N}(t)\mathcal{N}(\lambda)\sum_{m=1}^{N}\sum_{n=1}^{N}c_m c_n\cos(2\pi m f_0\lambda)\cos(2\pi n f_0 t)d\lambda dt\right], \\
&= \int_{\lambda=0}^{T_s}\int_{t=0}^{T_b}\sum_{m=1}^{N}\sum_{n=1}^{N}c_m c_n E[\mathcal{N}(t)\mathcal{N}(\lambda)]d\lambda dt, \\
&= \int_{\lambda=0}^{T_s}\int_{t=0}^{T_b}\frac{NN_0}{2}\delta(t-\lambda)c_m c_n\cos(2\pi m f_0 t)\cos(2\pi n f_0 t)d\lambda dt, \\
&= \frac{NN_0}{2}\int_{t=0}^{T_b}c_n^2\cos^2(2\pi m f_0 t)dt, \\
&= \frac{NN_0}{4}\int_{t=0}^{T_s}[1+\cos(4\pi m f_0 t)]dt, \\
&= \frac{NN_0T_s}{4}.
\end{aligned} \tag{3.7}$$

The MAI from the kth user equals

$$\begin{aligned}
I^{(1,k)} &= \sqrt{\frac{2P}{N}}\Big\{\cos\varphi_k[a_{-1}^{(k)}\mathcal{R}_{u_1,u_k}(\tau_k)+a_0^{(k)}\widehat{\mathcal{R}}_{u_1,u_k}(\tau_k)] \\
&\quad -\sin\varphi_k[a_{-1}^{(k)}\mathcal{R}_{u_1,v_k}(\tau_k)+a_0^{(k)}\widehat{\mathcal{R}}_{u_1,v_k}(\tau_k)]\Big\},
\end{aligned} \tag{3.8}$$

where

$$\mathcal{R}_{x,y}(\tau)=\int_0^{\tau}x(t)y(t-\tau)dt \quad \text{and} \quad \widehat{\mathcal{R}}_{x,y}(\tau)=\int_{\tau}^{T_s}x(t)y(t-\tau)dt. \tag{3.9}$$

After some manipulations, the expression in (3.8) can be rewritten as:

$$I^{(1,k)}=\sqrt{\frac{2P}{N}}\sum_{n=1}^{N}\left\{\mathcal{A}_n\sin\frac{2\pi n\tau_k}{T_s}+\mathcal{B}_n\cos\frac{2\pi n\tau_k}{T_s}\right\}, \tag{3.10}$$

where

$$\begin{aligned}
\mathcal{A}_n &= \frac{c_n^{(k)}c_n^{(1)}\sin\psi_k}{2}\left\{a_{-1}^{(k)}\tau_k+a_0^{(k)}[T_s-\tau_k]\right\} \\
&\quad +\frac{T_s\cos\psi_k[a_{-1}^{(k)}-a_0^{(k)}]}{2\pi}\left\{\sum_{\substack{i=1\\ i\neq n}}^{N}\frac{n[c_n^{(k)}c_i^{(1)}+c_n^{(k)}c_n^{(1)}]}{n^2-i^2}+\frac{c_n^{(k)}c_n^{(1)}}{2n}\right\},
\end{aligned} \tag{3.11}$$

and

$$\begin{aligned}
\mathcal{B}_n &= \frac{c_n^{(k)}c_n^{(1)}\cos\psi_k}{2}\left\{a_{-1}^{(k)}\tau_k+a_0^{(k)}[T_s-\tau_k]\right\} \\
&\quad +\frac{T_s\sin\psi_k}{2\pi}\left\{[a_{-1}^{(k)}-a_0^{(k)}]\sum_{\substack{i=1\\ i\neq n}}^{N}\frac{nc_n^{(k)}c_i^{(1)}+ic_n^{(1)}c_i^{(k)}}{i^2-n^2}-\frac{c_n^{(k)}c_n^{(1)}a_0^{(k)}}{2n}\right\}.
\end{aligned} \tag{3.12}$$

It is interesting to note that the interference term in MC-CDMA is different from those in DS-CDMA [16]. From (3.10), we can see that the aperiodic cross-correlation of the signature sequences is no longer the basic metric of the interference calculation. It is because we are transmitting a combination of sinusoids in MC-CDMA instead of a train of '+' and '−' rectangular chips across the time. This is the major difference between MC-CDMA and DS-CDMA in the signal design point of view.

Gaussian approximation (G.A.) is then used to estimate the probability of error in the proposed MC-CDMA system. For simplicity, we assume $a_j^{(k)}$ is equally distributed between '+1' and '−1' for $k \in \{2, \ldots, M\}$ and the random variables τ_k, $a_{j-1}^{(k)}$ and $a_j^{(k)}$ are independent. Without loss of generality, we consider only $a_1^{(k)} = +1$ since the case for $a_1^{(k)} = -1$ can be similarly determined by symmetry [16]. In the analysis, *random* signature sequences are assumed in operation, and the average value of the variance in the MC-CDMA system is found to be

$$E[Var\{I^{(1,k)}\}] = \frac{PT_s^2}{4\pi^2 N}\left\{\left[\sum_{n=1}^{N}\sum_{\substack{i=1 \\ i\neq n}}^{N}\frac{3n^2+i^2}{(n^2-i^2)^2}\right] + \frac{2\pi^2}{3}\right\}. \tag{3.13}$$

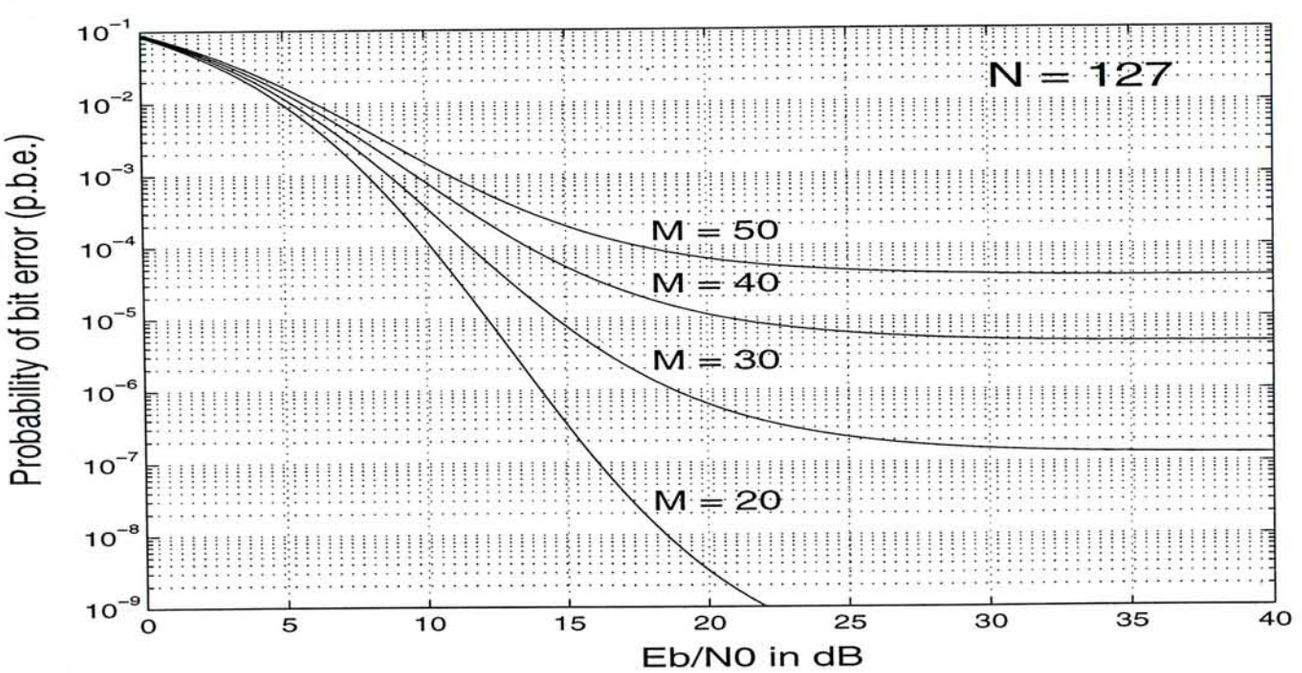

Figure 3.6: General performance of the MC-CDMA System.

By assuming the interference among all other users are independent, the total interference power would simply be the summation of every $Var\{I^{(1,k)}\}$. The signal-to-noise

and interference ratio SNIR at the RCVR$^{(1)}$ is then approximated as

$$\text{SNIR} = \frac{NPT_s^2/2}{\frac{(M-1)PT_s^2}{4\pi^2 N}\left\{\left[\sum_{n=1}^{N}\sum_{\substack{i=1\\ i\neq n}}^{N}\frac{3n^2+i^2}{(n^2-i^2)^2}\right]+\frac{2\pi^2}{3}\right\}+\frac{NN_0T_s}{4}}. \tag{3.14}$$

After simplification, we have

$$\text{SNIR} \approx \frac{1}{\frac{M-1}{2N^2\pi^2}\left\{\left[\sum_{n=1}^{N}\sum_{\substack{i=1\\ i\neq n}}^{N}\frac{3n^2+i^2}{(n^2-i^2)^2}\right]+\frac{2\pi^2}{3}\right\}+\frac{N_0}{2E_b}}, \tag{3.15}$$

where E_b is transmitted signal energy in one symbol period, PT_s. The *standard* Gaussian approximation formula of the proposed MC-CDMA system is therefore given by $P_e \approx Q(\sqrt{\text{SNIR}})$, where $Q(x)$ is the complementary error function. The general performance curve is shown in Figure 3.6 and the capacity of the MC-CDMA system with different number of carriers under the constraint of p.b.e. $< 10^{-3}$ is shown in Figure 3.7.

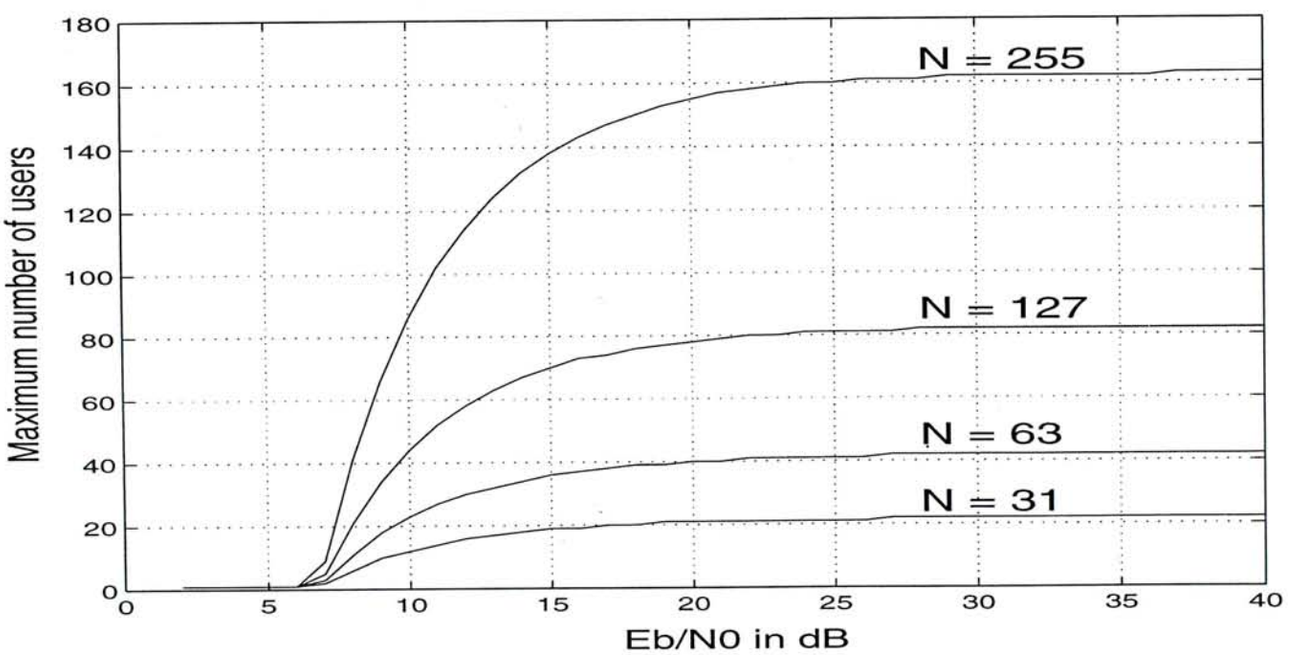

Figure 3.7: Capacity of the MC-CDMA system with $P_e < 10^{-3}$.

The system performance is simulated with N equals 15, 31 and 63. The ratio of bit energy to noise power (E_b/N_0) is set at 10dB and the results are shown in Figure 3.8. From the figure, we can see that Gaussian approximation can fairly estimate the system performance for considerable number of users.

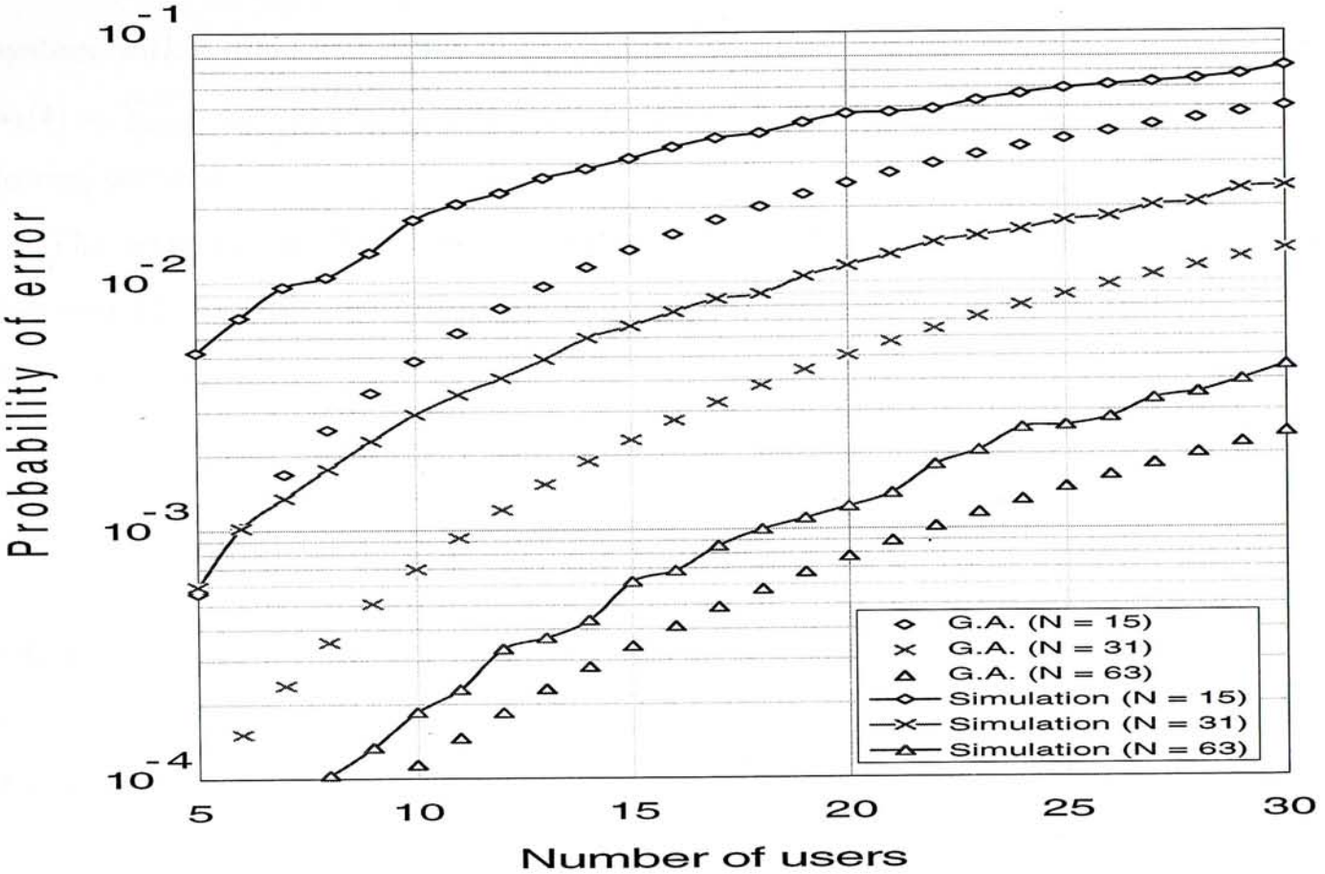

Figure 3.8: Error probability of MC-CDMA system.

It is well-known that the simple rule-of-thumb on the capacity of DS-SS system is given by $\frac{1}{3}$(*spreading factor*) [17]. From Figure 3.7, we see that the maximum number of users can be supported in the proposed system is greater than that of DS-SS system for a given performance measure (e.g. probability of error).

3.2.2 Fading Channel

The analysis of the fading effects on multicarrier system is not a new topic [18]. However, nearly most of the research papers focused on the case of slowly varying frequency selective fading channel and simply neglect the effect of Doppler spread. In the following analysis, time selective fading channel is assumed, which is a *dual* of the commonly used frequency selective fading channel [19]. Although the analysis of DS-SS system under time-selective fading channel was available in literature long time ago [20], yet the channel covariance functions used are not widely acceptable for mobile radio communication in practice. It is therefore worthwhile to analyze the proposed MC-CDMA

system with a modified channel covariance function. For the sake of clarity, we let $u_k(t) = \sum_{m=1}^{N} c_m^{(k)} \cos\left(\frac{2\pi mt}{T_s}\right)$ and $v_k(t) = \sum_{n=1}^{N} c_n^{(k)} \sin\left(\frac{2\pi nt}{T_s}\right)$ in the analysis of the following sections.

The received signal at every instant is first considered, i.e. the data stream of the kth user at the baseband $a^{(k)}(t)$ equals $\sum_{j=-\infty}^{\infty} a_j^{(k)} p_{T_s}(t - jT_s)$, and the received signal $r(t)$ can be described as:

$$\begin{aligned} r(t) &= \sum_{k=1}^{M-1} \gamma_k [\cos(2\pi f_c t + \varphi_k) \int_{-\infty}^{\infty} \beta_k(\tau, t) s_{\mathbf{I}}^{(k)}(t-\tau) d\tau \\ &\quad - \sin(2\pi f_c t + \varphi_k) \int_{-\infty}^{\infty} \beta_k(\tau, t) s_{\mathbf{Q}}^{(k)}(t-\tau) d\tau] + \mathcal{N}(t), \end{aligned} \tag{3.16}$$

where γ_k and β_k are the transmission coefficient and the baseband equivalent zero mean complex Gaussian fading characteristic experienced from the kth user respectively. The covariance function for the fading process in a WSSUS channel is

$$\begin{aligned} \Psi_k(\tau, \sigma; t, s) &\cong \frac{1}{2} E\{\beta_k(\tau, t) \beta_k^*(\sigma, s)\}, \\ &= \rho_k(\tau, t-s) \delta(\tau - \sigma). \end{aligned} \tag{3.17}$$

For time-selective fading channel, the above function is only dependent on $t - s$ (ς say) and assuming all the users observe the same fading characteristics, we have [20]:

$$\Psi_k(\tau, \sigma; t, s) \approx \rho(\varsigma). \tag{3.18}$$

In the propagation model provided by Clarke, the covariance function in (3.18) may be described as [21]:

$$\rho(\varsigma) = \frac{1}{2} J_0(2\pi f_m \varsigma), \tag{3.19}$$

where J_0 is the Bessel function of the first kind with zero-order and f_m is the maximum Doppler spread of the detected signal. As the argument of the Bessel function in (3.19) is usually on the order $10^{-3} \sim 10^{-4}$, the covariance function can be approximated as [22, 23]:

$$\rho(\varsigma) = \frac{1}{2}[1 - (\pi f_m \varsigma)^2]. \tag{3.20}$$

The demodulated signal at the intended (1st) receiver is:

$$Z^{(1)} = S^{(1)} + \tilde{F}_{\mathrm{Re}}^{(1)} + \sum_{k=2}^{M} [\tilde{I}_{\mathrm{Re}}^{(1,k)} + I^{(1,k)}] + N_D, \tag{3.21}$$

The above equation resembles (3.5), where $\tilde{F}^{(1)}_{\mathrm{Re}}$ and $\tilde{I}^{(1,k)}_{\mathrm{Re}}$ equal the real part of $\tilde{F}^{(1)}$ and $\tilde{I}^{(1,k)}$ respectively. The two additional terms $\tilde{F}^{(1)}$ and $\tilde{I}^{(1,k)}$ are respectively given by:

$$\tilde{F}^{(1)} = \gamma_1 \sqrt{\frac{2P}{N}} \int_0^{T_s} \int_{-\infty}^{\infty} \beta_1(\tau, t) h_{\mathbf{I}}^{(1,1)}(\tau;t) d\tau dt, \tag{3.22}$$

and

$$\begin{aligned} \tilde{I}^{(1,k)} &= \sqrt{\frac{2P}{N}} \sum_{k=2}^{M} \gamma_k \int_0^{T_s} \int_{-\infty}^{\infty} \beta_k(\tau, t-\tau_k)[\cos\varphi_k \\ &\quad \cdot h_{\mathbf{I}}^{(1,k)}(\tau_k+\tau;t) - \sin\varphi_k h_{\mathbf{Q}}^{(1,k)}(\tau_k+\tau;t)] d\tau dt, \end{aligned} \tag{3.23}$$

where

$$\begin{cases} h_{\mathbf{I}}^{(1,k)}(\tau_k+\tau;t) &= a^{(k)}(t-\tau) u_1(t) u_k(t-\tau) \\ h_{\mathbf{Q}}^{(1,k)}(\tau_k+\tau;t) &= a^{(k)}(t-\tau) u_1(t) v_k(t-\tau) \end{cases} . \tag{3.24}$$

The desired signal power $S^{(1)}$, unfaded interference $I^{(1,k)}$ and the noise power are the same as those obtained in the previous section and would not be derived here, whereas the variance of the fading component is [20]:

$$\begin{aligned} Var\{\tilde{F}^{(1)}_{\mathrm{Re}}\} = E[\tilde{F}^{(1)}_{\mathrm{Re}}]^2 &= \frac{1}{2} E[\tilde{F}^{(1)}_{\mathrm{Re}}]^2 + \frac{1}{2} E[conj(\tilde{F}^{(1)}) \times \tilde{F}^{(1)}], \\ &= \frac{1}{2} E|\tilde{F}^{(1)}|^2 \end{aligned} \tag{3.25}$$

The term $E[\tilde{F}^{(1)}_{\mathrm{Re}}]^2$ in (3.25) vanishes as the fading of the channel is of wide sense stationary uncorrelated scattering (WSSUS). The variance in (3.25) can then be expressed as:

$$Var\{\tilde{F}^{(1)}_{\mathrm{Re}}\} = \frac{2P}{N} \int_0^{T_s} \int_0^{T_s} \int_{-\infty}^{\infty} \gamma_1^2 \rho_1(\tau, t-s) g_1(\tau; t, s) d\tau dt ds, \tag{3.26}$$

where $g_1(\tau; t, s) = h_{\mathbf{I}}^{(1,1)}(\tau; t) h_{\mathbf{I}}^{(1,1)}(\tau; s)$. The channel covariance function of time-selective fading channel is shown to be [20]: $\rho_i(\tau, t-s) = \rho_i(0, t-s)\delta(\tau)$. We may simply denote it as $\rho(\varsigma)$. The equation (3.25) can then be expressed as:

$$Var\{\tilde{F}^{(1)}_{\mathrm{Re}}\} = \frac{2P\gamma_1^2}{N} \int_0^{T_s} \int_0^{T_s} \rho(\varsigma) a^{(k)}(t) a^{(k)}(s) [u^{(k)}(t) u^{(k)}(s)]^2 dt ds. \tag{3.27}$$

Using $\varsigma = t - s$, the region of integration is shown as Figure 3.9.

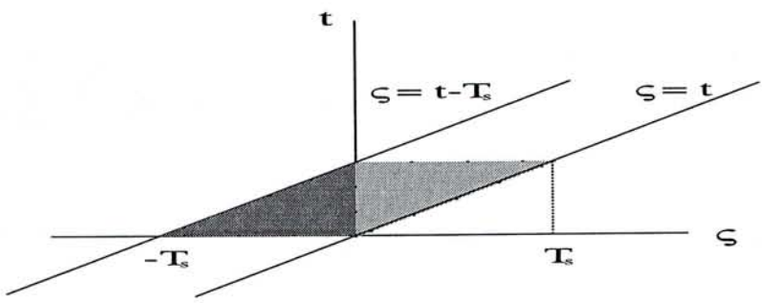

Figure 3.9: Region of integration in the $\varsigma - t$ plane.

Hence,

$$Var\{\tilde{F}_{\mathrm{Re}}^{(1)}\} = \frac{2P\gamma_1^2}{N}\Big\{\int_0^{T_s}\int_{\varsigma}^{T_s}\rho(\varsigma)[u^{(k)}(t)u^{(k)}(t-\varsigma)]^2 dtd\varsigma + \int_{-T_s}^{0}\int_{0}^{\varsigma+T_s}\rho(\varsigma)[u^{(k)}(t)u^{(k)}(t-\varsigma)]^2 dtd\varsigma\Big\}. \quad (3.28)$$

Let the first term and the second term of the bracket in (3.28) be $\mathcal{F}_A$ and $\mathcal{F}_B$ respectively. Then, we have

$$\begin{aligned}\mathcal{F}_A = \sum_{\nu=1}^{N}\sum_{n=1}^{N}\int_0^{T_s}\rho(\varsigma)\int_{\varsigma}^{T_s}\Big\{\Big[&\cos^2(2\pi n f_0 t) \\ &+2\sum_{\substack{m=1\\ \neq n}}^{N} c_m c_n \cos(2m\pi f_0 t)\cos(2n\pi f_0 t)\Big] \times \Big[\cos^2(2\pi\mu f_0(t-\varsigma)) \\ &+2\sum_{\substack{\mu=1\\ \neq \nu}}^{N} c_\mu c_\nu \cos(2\mu\pi f_0(t-\varsigma))\cos(2\nu\pi f_0(t-\varsigma))\Big]\Big\} dtd\varsigma. \end{aligned} \quad (3.29)$$

which can be expressed as:

$$\begin{aligned}\mathcal{F}_A = \sum_{\nu=1}^{N}\sum_{n=1}^{N}\int_0^{T_s}\rho(\varsigma)\Big[&\mathcal{F}_{A,1}(n,\nu,\varsigma) + 2\sum_{\substack{\mu=1\\ \neq \nu}}^{N} c_\mu c_\nu \mathcal{F}_{A,2}(n,\mu,\nu,\varsigma) + 2\sum_{\substack{m=1\\ \neq n}}^{N} c_m c_n \\ &\cdot\mathcal{F}_{A,3}(m,n,\nu,\varsigma) + 4\sum_{\substack{m=1\\ \neq n}}^{N}\sum_{\substack{\mu=1\\ \neq \nu}}^{N} c_m c_n c_\mu c_\nu \mathcal{F}_{A,4}(m,n,\mu,\nu,\varsigma)\Big] d\varsigma. \end{aligned} \quad (3.30)$$

The components constitute the $\mathcal{F}_A$ in (3.30) are the following integrals

$$\begin{cases} \mathcal{F}_{A,1}(n,\nu,\varsigma) = \int_{\varsigma}^{T_s}\cos^2(2\pi n f_0 t)\cos^2(2\pi\nu f_0(t-\varsigma))dt \\ \mathcal{F}_{A,2}(n,\mu,\nu,\varsigma) = \int_{\varsigma}^{T_s}[\cos^2(2\pi n f_0 t)\cos(2\pi\mu f_0(t-\varsigma))\cos(2\pi\nu f_0(t-\varsigma))]dt \\ \mathcal{F}_{A,3}(m,n,\nu,\varsigma) = \int_{\varsigma}^{T_s}\cos^2(2\pi\nu f_0(t-\varsigma))\cos(2\pi m f_0 t)\cos(2\pi n f_0 t)dt \\ \mathcal{F}_{A,4}(m,n,\mu,\nu,\varsigma) = \int_{\varsigma}^{T_s}\cos(2\pi m f_0 t)\cos(2\pi n f_0 t) \\ \qquad\qquad \cdot\cos(2\pi\mu f_0(t-\varsigma))\cos(2\pi\nu f_0(t-\varsigma))dt \end{cases} \quad (3.31)$$

Similarly,

$$\mathcal{F}_B = \sum_{\nu=1}^{N}\sum_{n=1}^{N}\int_0^{T_s}\rho(\varsigma)\Big[\mathcal{F}_{B,1}(n,\nu,\varsigma)+2\sum_{\substack{\mu=1\\\neq\nu}}^{N}c_\mu c_\nu\mathcal{F}_{B,2}(n,\mu,\nu,\varsigma)+2\sum_{\substack{m=1\\\neq n}}^{N}c_m c_n \cdot\mathcal{F}_{B,3}(m,n,\nu,\varsigma)+4\sum_{\substack{m=1\\\neq n}}^{N}\sum_{\substack{\mu=1\\\neq\nu}}^{N}c_m c_n c_\mu c_\nu\mathcal{F}_{B,4}(m,n,\mu,\nu,\varsigma)\Big]d\varsigma, \tag{3.32}$$

where all the components $\mathcal{F}_{B,i}(\ldots,\varsigma')$ equal $\mathcal{F}_{A,i}(\ldots,\varsigma)$ for $i\in\{1,\ldots,4\}$ with the substitution of $\varsigma'=-\varsigma$. As the covariance function of the time selective fading channel is an even function, then the variance in (3.26) equals:

$$\begin{aligned}Var\{\tilde{F}^{(1)}_{\mathrm{Re}}\} = \frac{4P\gamma_1^2}{N}\sum_{\nu=1}^{N}\sum_{n=1}^{N}\int_0^{T_s}\rho(\varsigma)\Big[&\mathcal{F}_{A,1}(n,\nu,\varsigma)+2\sum_{\substack{\mu=1\\\neq\nu}}^{N}c_\mu c_\nu\mathcal{F}_{A,2}(n,\mu,\nu,\varsigma)\\&+2\sum_{\substack{m=1\\\neq n}}^{N}c_m c_n\mathcal{F}_{A,3}(m,n,\nu,\varsigma)\\&+4\sum_{\substack{m=1\\\neq n}}^{N}\sum_{\substack{\mu=1\\\neq\nu}}^{N}c_m c_n c_\mu c_\nu\mathcal{F}_{A,4}(m,n,\mu,\nu,\varsigma)\Big]d\varsigma.\end{aligned} \tag{3.33}$$

After evaluating the fading component and average it over the random signature sequences, we have:

$$\begin{aligned}E\left[Var\{\tilde{F}^{(1)}_{\mathrm{Re}}\}\right] &= \frac{4\gamma_1^2P}{N}\overline{\int_0^{T_s}\int_\varsigma^{T_s}\rho(\varsigma)[u_1(t)u_1(t-\varsigma)]^2dtd\varsigma},\\ &= \frac{4\gamma_1^2P}{N}\int_0^{T_s}\rho(\varsigma)\Bigg\{\frac{N(T_s-\varsigma)}{4}+\sum_{n=1}^{N}\Bigg[\frac{T_s-\varsigma}{8}\cos\left(\frac{4n\pi\varsigma}{T_s}\right)\\&\quad-\frac{5T_s}{32n\pi}\sin\left(\frac{4n\pi\varsigma}{T_s}\right)+T_s\sum_{\substack{l=1\\\neq n}}^{N}\frac{1}{16\pi nl[n^2-l^2]}\Big[n(2l^2-n^2)\\&\quad\cdot\sin\left(\frac{4\pi l\varsigma}{T_s}\right)+l(l^2-2n^2)\sin\left(\frac{4\pi n\varsigma}{T_s}\right)\Big]-\frac{1}{nl\pi}\Big[l\cos\left(\frac{2l\pi\varsigma}{T_s}\right)\\&\quad\cdot\sin\left(\frac{2n\pi\varsigma}{T_s}\right)+n\cos\left(\frac{2\pi n\varsigma}{T_s}\right)\sin\left(\frac{2\pi l\varsigma}{T_s}\right)\Big]+\frac{1}{2\pi(l^2-n^2)}\\&\quad\cdot\Big[(n-l)\sin\left(\frac{2\pi(l+n)\varsigma}{T_s}\right)-(l+n)\sin\left(\frac{2\pi(l-n)\varsigma}{T_s}\right)\Big]\\&\quad+2\Big(1-\frac{\varsigma}{T_s}\Big)\cos\left(\frac{2\pi l\varsigma}{T_s}\right)\cos\left(\frac{2\pi n\varsigma}{T_s}\right)\Bigg]\Bigg\}d\varsigma.\end{aligned} \tag{3.34}$$

By (3.18), (3.24), (3.26) and the substitution of $\xi=f_mT_s$, it can be shown that

$$E\left[Var\{\tilde{F}^{(1)}_{\mathrm{Re}}\}\right]=\frac{4\gamma_1^2PT_s^2}{N}\left\{\frac{N^2[6-(\pi\xi)^2]}{96}-\xi^2\sum_{n=1}^{N}\left[\frac{1}{64n^2}+\sum_{\substack{l=1\\\neq n}}^{N}\frac{n^2+l^2}{128n^2l^2}\right]\right\}. \tag{3.35}$$

On the other hand, the variance of the MAI can be easily derived. The effect of the multiple access interference (MAI) is considered as follows:

$$Var\{\tilde{I}_{\mathrm{Re}}^{(1,k)}\} = \frac{2P}{N}\sum_{k=2}^{M}\gamma_k^2\int_0^{T_s}\int_0^{T_s}\rho(t-s)E\Big\{\Big[\cos\varphi_k h_{\mathbf{I}}^{(1,k)}(\tau_k,t) - \sin\varphi_k \cdot h_{\mathbf{Q}}^{(1,k)}(\tau_k,t)\Big]\times\Big[\cos\varphi_k h_{\mathbf{I}}^{(1,k)}(\tau_k,s) - \sin\varphi_k h_{\mathbf{Q}}^{(1,k)}(\tau_k,s)\Big]\Big\}dtds. \quad (3.36)$$

Let the expression in the bracket of (3.36) be $G(\tau_k,t,s)$, which can be expanded as:

$$\begin{aligned} E\{G(\tau_k,t,s)\} &= E\Big\{a^{(k)}(t-\tau_k)a^{(k)}(s-\tau_k)u_1(t)u_1(s)\Big[u_k(t-\tau_k)\cos\varphi_k - v_k(t-\tau_k)\cdot\sin\varphi_k\Big]\times\Big[u_k(s-\tau_k)\cos\varphi_k - v_k(s-\tau_k)\sin\varphi_k\Big]\Big\}, \\ &= E\Big\{a^{(k)}(t-\tau_k)a^{(k)}(s-\tau_k)u_i(t)u_i(s)\Big[u_k(t-\tau_k)u_k(s-\tau_k)\cos^2\varphi_k \\ &\quad -\Big(u_k(t-\tau_k)v_k(s-\tau_k)+u_k(s-\tau_k)v_k(t-\tau_k)\Big)\sin\varphi_k\cos\varphi_k \\ &\quad +v_k(t-\tau_k)v_k(s-\tau_k)\sin^2\varphi_k\Big]\Big\}. \end{aligned} \quad (3.37)$$

As φ_k and τ_k are independent while $u_1(t)$ and $u_1(s)$ are known, we first take the expectation of the φ_k so that equation (3.37) becomes

$$E\{G(\tau_k,t,s)\} = \frac{u_1(t)u_1(s)}{2}\int_0^{T_s}\frac{\overline{a^{(k)}(t-\tau_k)a^{(k)}(s-\tau_k)}}{T_s}\Big[u_k(t-\tau_k)u_k(s-\tau_k) + v_k(t-\tau_k)v_k(s-\tau_k)\Big]d\tau_k, \quad (3.38)$$

where

$$\begin{cases} a^{(k)}(t-\tau_k) &= \sum_{x=-\infty}^{\infty}a_x^{(k)}p_{T_s}(t-\tau_k-xT_s) \\ a^{(k)}(s-\tau_k) &= \sum_{y=-\infty}^{\infty}a_y^{(k)}p_{T_s}(s-\tau_k-yT_s) \end{cases}. \quad (3.39)$$

In equation (3.38), $E\{G(\tau_k,t,s)\}$ exists only if $|t-s|\le T_s$ and $x=y$ in (3.39). For simplicity, assume $x=y=0$ (say), and the product $a^{(k)}(t-\tau_k)\cdot a^{(k)}(s-\tau_k)$ is then governed by the contribution of the components.

$$p_{T_s}(\varepsilon-\tau_k) = \begin{cases} 1\ , & \varepsilon-T_s\le\tau_k\le t \\ 0\ , & otherwise \end{cases} \quad (\text{where } \varepsilon = s \text{ or } t). \quad (3.40)$$

Case 1: $t-s\ge 0$

In this case, (3.38) becomes,

$$\begin{aligned} E\{G(\tau_k,t,s)\} &= \frac{u_1(t)u_1(s)}{2T_s}\int_{t-T_s}^{s}\Big[u_k(t-\tau_k)u_k(s-\tau_k)+v_k(t-\tau_k)v_k(s-\tau_k)\Big]d\tau_k, \\ &= \frac{u_1(t)u_1(s)}{2T_s}\int_{t-T_s}^{s}\Big[u_k(t-\tau_k)u_k(t-\varsigma-\tau_k) \\ &\quad +v_k(t-\tau_k)v_k(t-\varsigma-\tau_k)\Big]d\tau_k, \\ &= \frac{u_1(t)u_1(s)}{2T_s}\int_{\varsigma}^{T_s}\Big[u_k(\alpha)u_k(\alpha-\varsigma)+v_k(\alpha)v_k(\alpha-\varsigma)\Big]d\alpha, \ (\alpha=t-\tau_k) \\ &= \frac{u_1(t)u_1(s)}{2T_s}\Big[\widehat{\mathcal{R}}_{u_k,u_k}(\varsigma)+\widehat{\mathcal{R}}_{v_k,v_k}(\varsigma)\Big]. \end{aligned} \tag{3.41}$$

Case 2: $t-s<0$

Using the similar technique as in *Case 1*, we have:

$$E\{G(\tau_k,t,s)\} = \frac{u_1(t)u_1(s)}{2T_s}\Big[\widehat{\mathcal{R}}_{u_k,u_k}(-\varsigma)+\widehat{\mathcal{R}}_{v_k,v_k}(-\varsigma)\Big]. \tag{3.42}$$

In (3.41), $\widehat{\mathcal{R}}_{u_k,u_k}(\varsigma)$ and $\widehat{\mathcal{R}}_{v_k,v_k}(-\varsigma)$ equal

$$\begin{cases} \widehat{\mathcal{R}}_{u_k,u_k}(\varsigma) &= \sum_{n=1}^{N}\sum_{m=1}^{N} c_m^{(k)}c_n^{(k)}\int_{\varsigma}^{T_s}\cos(2\pi mt/T_s)\cos(2\pi n(t-\varsigma)/T_s)dt, \\ \widehat{\mathcal{R}}_{v_k,v_k}(\varsigma) &= \sum_{n=1}^{N}\sum_{m=1}^{N} c_m^{(k)}c_n^{(k)}\int_{\varsigma}^{T_s}\sin(2\pi mt/T_s)\sin(2\pi n(t-\varsigma)/T_s)dt. \end{cases} \tag{3.43}$$

For simplicity $\widehat{\mathcal{R}}_{u_k,u_k}(\varsigma)$ and $\widehat{\mathcal{R}}_{v_k,v_k}(\varsigma)$ will be denoted as $\widehat{\mathcal{R}}_{u_k}(\varsigma)$ and $\widehat{\mathcal{R}}_{v_k}(\varsigma)$ respectively. It can be observed that both the aperiodic autocorrelation functions of $u_k(t)$ and $v_k(t)$ discussed above are odd function of ς. We will therefore use this property to derive the MAI. The equation (3.36) is rewritten as:

$$Var\{\tilde{I}_{\mathrm{Re}}^{(1,k)}\} = \frac{P}{NT_s}\sum_{k=2}^{M}\gamma_k^2\int_0^{T_s}\int_0^{T_s}\rho(t-s)u_1(t)u_1(s)\Big\{\widehat{\mathcal{R}}_{u_k}(\varsigma)+\widehat{\mathcal{R}}_{v_k}(\varsigma)\Big\}dtds. \tag{3.44}$$

Similar to the derivation of $Var\{\tilde{F}_{\mathrm{Re}}^{(1)}\}$ and as described pictorially as in Figure 3.9, we have:

$$\begin{aligned} Var\{\tilde{I}_{\mathrm{Re}}^{(1,k)}\} &= \frac{P}{NT_s}\sum_{k=2}^{M}\gamma_k^2\Big\{\int_0^{T_s}\int_{\varsigma}^{T_s}\rho(\varsigma)u_1(t)u_1(t-\varsigma)\Big[\widehat{\mathcal{R}}_{u_k}(\varsigma)+\widehat{\mathcal{R}}_{v_k}(\varsigma)\Big]dtd\varsigma \\ &\quad +\int_{-T_s}^{0}\int_{0}^{\varsigma+T_s}\rho(\varsigma)u_1(t)u_1(t-\varsigma)\Big[\widehat{\mathcal{R}}_{u_k}(-\varsigma)+\widehat{\mathcal{R}}_{v_k}(-\varsigma)\Big]dtd\varsigma\Big\}, \\ &= \frac{P}{NT_s}\sum_{k=2}^{M}\gamma_k^2\Big\{\int_0^{T_s}\rho(\varsigma)\Big[\widehat{\mathcal{R}}_{u_k}(\varsigma)+\widehat{\mathcal{R}}_{v_k}(\varsigma)\Big]\cdot\Big[\int_{\varsigma}^{T_s}u_1(t)u_1(t-\varsigma)dt\Big]d\varsigma, \end{aligned}$$

$$
\begin{aligned}
&+\int_0^{T_s}\rho(\varsigma)\big[\widehat{\mathcal{R}}_{u_k}(-\varsigma)+\widehat{\mathcal{R}}_{v_k}(-\varsigma)\big]\cdot\Big[\int_0^{\varsigma+T_s}u_1(t)u_1(t-\varsigma)dt\Big]d\varsigma\Big\},\\
=\;&\frac{P}{NT_s}\sum_{k=2}^{M}\gamma_k^2\Big\{\int_0^{T_s}\rho(\varsigma)\big[\widehat{\mathcal{R}}_{u_k}(\varsigma)+\widehat{\mathcal{R}}_{v_k}(\varsigma)\big]\widehat{\mathcal{R}}_{u_1}(\varsigma)d\varsigma\\
&+\int_{-T_s}^{0}\rho(\varsigma)\big[\widehat{\mathcal{R}}_{u_k}(-\varsigma)+\widehat{\mathcal{R}}_{v_k}(-\varsigma)\big]\widehat{\mathcal{R}}_{u_1}(-\varsigma)d\varsigma\Big\},\\
=\;&\frac{P}{NT_s}\sum_{k=2}^{M}\gamma_k^2\Big\{\int_0^{T_s}\rho(\varsigma)\big[\widehat{\mathcal{R}}_{u_k}(\varsigma)+\widehat{\mathcal{R}}_{v_k}(\varsigma)\big]\widehat{\mathcal{R}}_{u_1}(\varsigma)d\varsigma\\
&-\int_{T_s}^{0}\rho(\varsigma')\big[\widehat{\mathcal{R}}_{u_k}(\varsigma')+\widehat{\mathcal{R}}_{v_k}(\varsigma')\big]\widehat{\mathcal{R}}_{u_1}(\varsigma')d\varsigma'\Big\},\\
=\;&\frac{2P}{NT_s}\sum_{k=2}^{M}\gamma_k^2\int_0^{T_s}\rho(\varsigma)\widehat{\mathcal{R}}_{u_1}(\varsigma)\cdot\big[\widehat{\mathcal{R}}_{u_k}(\varsigma)+\widehat{\mathcal{R}}_{v_k}(\varsigma)\big]d\varsigma. \qquad (3.45)
\end{aligned}
$$

Now, consider the average value of the expression in (3.45), which is:

$$
E\big[Var\{\tilde{I}_{\mathrm{Re}}^{(1,k)}\}\big]=\frac{2P}{NT_s}\sum_{k=2}^{M}\gamma_k^2\int_0^{T_s}\rho(\varsigma)\overline{\widehat{\mathcal{R}}_{u_1}(\varsigma)\big[\widehat{\mathcal{R}}_{u_k}(\varsigma)+\widehat{\mathcal{R}}_{v_k}(\varsigma)\big]}d\varsigma. \qquad (3.46)
$$

We first evaluate the expression $\overline{\widehat{\mathcal{R}}_{u_1}(\varsigma)[\widehat{\mathcal{R}}_{u_k}(\varsigma)+\widehat{\mathcal{R}}_{v_k}(\varsigma)]}$, which equals

$$
\begin{aligned}
\overline{\widehat{\mathcal{R}}_{u_1}(\varsigma)[\widehat{\mathcal{R}}_{u_k}(\varsigma)+\widehat{\mathcal{R}}_{v_k}(\varsigma)]}\;=\;&\frac{T_s-\varsigma}{2}\sum_{l=1}^{N}\sum_{n=1}^{N}\Big\{\cos\Big(\frac{2\pi l\varsigma}{T_s}\Big)\Big[(T_s-\varsigma)\cos\Big(\frac{2\pi l\varsigma}{T_s}\Big)\\
&-\frac{T_s}{2\pi n}\sin\Big(\frac{2\pi l\varsigma}{T_s}\Big)\Big]\Big\}. \qquad (3.47)
\end{aligned}
$$

By assuming the MAIs from different users are independent and all the γ_k $(2\le k\le M)$ are the same (γ say) for simplicity, the average interference power is:

$$
\begin{aligned}
E\big[Var\{\tilde{I}_{\mathrm{Re}}^{(1,k)}\}\big]\;=\;&\frac{\gamma^2(M-1)P}{NT_s}\int_0^{T_s}(T_s-\varsigma)[1-(\pi f_m\varsigma)^2]\sum_{l=1}^{N}\sum_{n=1}^{N}\Big\{\cos\Big(\frac{2\pi l\varsigma}{T_s}\Big)\\
&\cdot\Big[(T_s-\varsigma)\cos\Big(\frac{2\pi n\varsigma}{T_s}\Big)-\frac{T_s}{2\pi n}\sin\Big(\frac{2\pi n\varsigma}{T_s}\Big)\Big]\Big\}d\varsigma,\\
=\;&\frac{\gamma^2(M-1)P}{4NT_s}\int_0^{T_s}[1-(\pi f_m\varsigma)^2]\times\Big\{\sum_{l=1}^{N}\sum_{\substack{n=1\\ \neq l}}^{N}\Big[(T_s-\varsigma)^2\\
&\cdot\cos\Big(\frac{2\pi l\varsigma}{T_s}\Big)\cos\Big(\frac{2\pi n\varsigma}{T_s}\Big)-\frac{T_s(T_s-\dot{\varsigma})}{2n\pi}\cos\Big(\frac{2\pi l\varsigma}{T_s}\Big)\\
&\cdot\sin\Big(\frac{2\pi n\varsigma}{T_s}\Big)\Big]+\sum_{n=1}^{N}\Big[(T_s-\varsigma)^2\cos^2\Big(\frac{2\pi n\varsigma}{T_s}\Big)\\
&-\frac{T_s(T_s-\varsigma)}{2n\pi}\cos\Big(\frac{2\pi n\varsigma}{T_s}\Big)\sin\Big(\frac{2\pi n\varsigma}{T_s}\Big)\Big]\Big\}d\varsigma,
\end{aligned}
$$

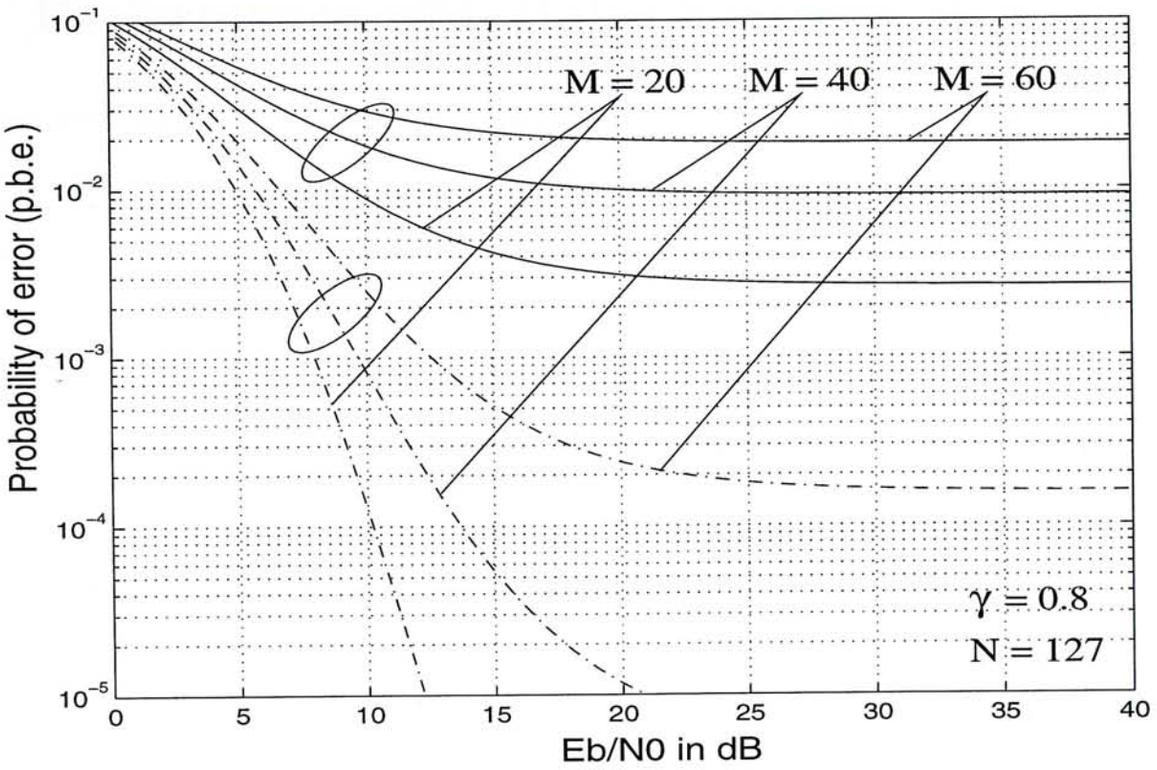

Figure 3.10: System performance in time-selective fading channel.

$$
\begin{aligned}
= \; & \frac{\gamma^2(M-1)PT_s^2}{8N}\sum_{n=1}^{N}\left\{\frac{2}{3}-(\pi\xi)^2\Big[\frac{1}{15}-\frac{3}{32(n\pi)^4}\Big]\right. \\
& +\sum_{\substack{l=1\\ \neq n}}^{N}\frac{1}{2\pi^4(n+l)^4(n-l)^4}\Big\{2\pi^2(n^2-l^2)^2(3l^2+n^2) \\
& +\xi^2\Big[12(l^4+6l^2n^2+n^4)+\pi^2(n^2-l^2)[8(l^4-n^4) \\
& \left.-3(3l^2+n^2)]+8\pi^4[(n^2+l^2)(n^2-l^2)^2]\Big]\Big\}\right\}. \qquad (3.48)
\end{aligned}
$$

The SNIR can then be obtained as:

$$
\mathrm{SNIR}=\frac{NPT_s^2/2}{E\left[Var\{\tilde{F}_{\mathrm{Re}}^{(1)}\}\right]+\sum_{k=2}^{M}E\left[Var\{\tilde{I}_{\mathrm{Re}}^{(1,k)}\}+Var\{I^{(1,k)}\}\right]+NN_0T_s/4}. \qquad (3.49)
$$

The performance of the MC-CDMA system under time-selective fading channel with $\xi = 0.001$ is shown in Figure 3.10, where the line group with dash-dot is the situation without the effect of fading and all the users are assumed to share the same transmission coefficient $\gamma = 0.8$. It is observed that the SNR saturates at around 15dB.

3.3 Performance with Pulse Shape

In the previous analysis, the symbol shape is assumed to be a rectangular pulse. However in practice, pulse shape is used to trim the out-of-band emissions. In DS-SS system, detail analysis was done [24], and the system performance with raised-cosine pulse shape was shown to be $P_e = Q\left[\left(\frac{M-1}{2N}(1-\frac{\alpha}{4})\right)^{-0.5}\right]$.

In multicarrier system, the pulse shape is done in the frequency domain (the *dual* of time domain) [25], and the raised-cosine filter becomes a window function given by:

$$\begin{cases} \frac{1}{2}[1+\cos\frac{\pi(t-\alpha T_s)}{\alpha T_s}] & : \quad 0 \le t \le \alpha T_s \\ 1 & : \quad \alpha T_s \le t \le T_s \\ \frac{1}{2}[1+\cos\frac{\pi(t-T_s)}{\alpha T_s}] & : \quad T_s \le t \le (1+\alpha)T_s \end{cases} \tag{3.50}$$

However, the close-form evaluation of the performance with pulse shape stated above may not be easily obtained for our system. A Monte-Carlo simulation is done with the assumption of Gaussian channel. The results are shown in Figure 3.11 with $N = 31$ and the roll-off factor is averaged over ± 0.05. The optimal probability of error can be obtained with $0.1 \le \alpha \le 0.3$.

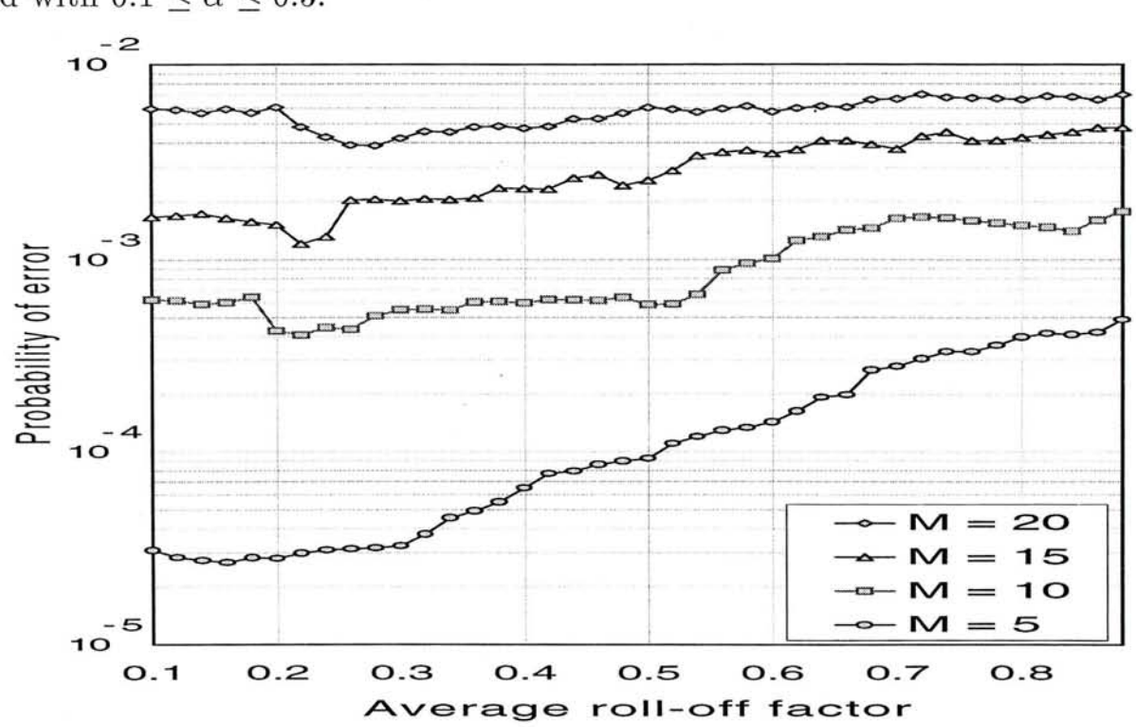

Figure 3.11: System performance with raised-cosine pulse shape.

3.4 Appendix

Derivation of the Multiple Access Interference

We provide the formal proof of the (3.13). Similar to the derivation of DS-CDMA [17], we claim that the interference component $I^{(1,k)}$ is of zero mean and the parameters τ_k, φ_k, $c_n^{(1)}$, $c_n^{(k)}$ and the data sequence are mutually independent, while the data sequence $\{\ldots, a_{j-1}, a_j, a_{j+1}, \ldots\}$ and the chips $\{\ldots, c_{n-1}, c_n, c_{n+1}, \ldots\}$ are further assumed to be identical independent distribution (i.i.d.) processes. Therefore:

$$Var\{I^{(1,k)}\} = E\Big\{ \left[I^{(1,k)}\right]^2 \Big\}. \tag{3.51}$$

Using (3.10), we have:

$$\begin{aligned}
\left[I^{(1,k)}\right]^2 \;=\; & \frac{2P}{N}\Bigg\{ \sum_{n=1}^{N} \mathcal{A}_n^2 \sin^2(2\pi n f_0 \tau_k) + \sum_{n=1}^{N} \mathcal{B}_n^2 \sin^2(2\pi n f_0 \tau_k) \\
& +2 \sum_{m=1}^{N} \sum_{\substack{n=1 \\ \neq m}}^{N} \mathcal{A}_m \mathcal{A}_n \sin(2\pi m f_0 \tau_k) \sin(2\pi n f_0 \tau_k) \\
& +2 \sum_{m=1}^{N} \sum_{\substack{n=1 \\ \neq m}}^{N} \mathcal{A}_m \mathcal{B}_n \sin(2\pi m f_0 \tau_k) \cos(2\pi n f_0 \tau_k) \\
& +2 \sum_{m=1}^{N} \sum_{\substack{n=1 \\ \neq m}}^{N} \mathcal{B}_m \mathcal{B}_n \cos(2\pi m f_0 \tau_k) \cos(2\pi n f_0 \tau_k) \Bigg\}.
\end{aligned} \tag{3.52}$$

where $\mathcal{A}_n$ and $\mathcal{B}_n$ are shown in (3.11) and (3.12) respectively. To avoid any inconvenience in reading this derivation, $\mathcal{A}_n$ and $\mathcal{B}_n$ are restated in the following.

$$\begin{aligned}
\mathcal{A}_n = & \frac{c_n^{(k)} c_n^{(1)} \sin\psi_k}{2} \Big\{ a_{-1}^{(k)} \tau_k + a_0^{(k)} [T_s - \tau_k] \Big\} \\
& + \frac{T_s \cos\psi_k [a_{-1}^{(k)} - a_0^{(k)}]}{2\pi} \Bigg\{ \sum_{\substack{i=1 \\ i \neq n}}^{N} \frac{n[c_n^{(k)} c_i^{(1)} + c_n^{(k)} c_n^{(1)}]}{n^2 - i^2} + \frac{c_n^{(k)} c_n^{(1)}}{2n} \Bigg\},
\end{aligned} \tag{3.53}$$

and

$$\begin{aligned}
\mathcal{B}_n = & \frac{c_n^{(k)} c_n^{(1)} \cos\psi_k}{2} \Big\{ a_{-1}^{(k)} \tau_k + a_0^{(k)} [T_s - \tau_k] \Big\} \\
& + \frac{T_s \sin\psi_k}{2\pi} \Bigg\{ [a_{-1}^{(k)} - a_0^{(k)}] \sum_{\substack{i=1 \\ i \neq n}}^{N} \frac{n c_n^{(k)} c_i^{(1)} + i c_n^{(1)} c_i^{(k)}}{i^2 - n^2} - \frac{c_n^{(k)} c_n^{(1)} a_0^{(k)}}{2n} \Bigg\}.
\end{aligned} \tag{3.54}$$

In order to evaluate the variance in (3.51), the expected values of the individual expressions in (3.52) should be obtained. Using our assumptions stated in the first paragraph and the fact that $|c_n^{(k)}| = 1$ for $k \in \{1, \ldots, M\}$, we can take the average of φ_k and τ_k and get:

$$
\begin{cases}
E[\mathcal{A}_n \sin^2(2\pi n f_0 \tau_k)] &= \frac{T_s^2}{8\pi^2}\left\{\left[\sum_{\substack{i=1\\ \neq n}}^{N} \frac{n[c_n^{(k)} c_i^{(1)} + c_i^{(k)} c_n^{(1)}]}{n^2 - i^2} + \frac{c_n^{(1)} c_n^{(k)}}{2n}\right]^2 + \frac{8n^2\pi^2 - 3}{24n^2}\right\}, \\
E[\mathcal{B}_n \cos^2(2\pi n f_0 \tau_k)] &= \frac{T_s^2}{8\pi^2}\left\{\left[\sum_{\substack{i=1\\ \neq n}}^{N} \frac{n c_n^{(1)} c_i^{(1)} + i c_n^{(k)} c_i^{(k)}}{2n(i^2 - n^2)} + \left(\frac{n c_n^{(k)} c_i^{(1)} + i c_n^{(1)} c_i^{(k)}}{i^2 - n^2}\right)^2\right] \right. \\
&\qquad \left. + \frac{8n^2\pi^2 + 6}{24n^2}\right\}, \\
E[A_m A_n \sin(2\pi m f_0 \tau_k) \sin(2\pi n f_0 \tau_k)] &= \frac{mnT_s^2}{4\pi^2(m^2 - n^2)}, \\
E[A_m B_n \sin(2\pi m f_0 \tau_k) \cos(2\pi n f_0 \tau_k)] &= \frac{T_s^2}{4\pi^2}\left\{\frac{m}{2(n^2 - m^2)} c_m^{(k)} c_n^{(k)}\left[c_m^{(1)} c_n^{(1)} \frac{n(m^2+2)}{4mn}\right.\right. \\
&\qquad \left. + \sum_{\substack{l=1\\ \neq m}}^{N} \frac{m}{m^2 - l^2} + \sum_{\substack{i=1\\ \neq n}}^{N} \frac{n c_i^{(1)} c_i^{(k)}}{i^2 - n^2}\right] \\
&\qquad - \frac{1}{8m}\left[\frac{2m+n}{2mn} + \sum_{\substack{i=1\\ \neq n}}^{N} \frac{n c_n^{(1)} c_i^{(1)} + i c_n^{(k)} c_i^{(k)}}{i^2 - n^2}\right. \\
&\qquad \left.\left. + \sum_{\substack{l=1\\ \neq m}}^{N} \frac{m(c_m^{(1)} c_l^{(1)} + c_l^{(k)} c_m^{(k)})}{m^2 - l^2}\right]\right\}, \\
E[B_m B_n \cos(2\pi m f_0 \tau_k) \cos(2\pi n f_0 \tau_k)] &= \frac{(m^2+n^2)T_s^2}{8\pi^2(m^2 - n^2)^2}.
\end{cases}
$$

After summing up the above expressions, substitute back terms into (3.52) and average the result over the signature sequence $\{c_n\}$, we have (3.13):

$$
E\left[Var\{I^{(1,k)}\}\right] = \frac{PT_s^2}{4\pi^2 N}\left\{\left[\sum_{n=1}^{N}\sum_{\substack{i=1\\ \neq n}}^{N} \frac{3n^2 + i^2}{(n^2 - i^2)^2}\right] + \frac{2\pi^2}{3}\right\}. \tag{3.55}
$$

Chapter 4

Signal Design Criteria for MC-CDMA System

In the previous analysis, we can see that in a MC-CDMA system the fundamental constituent of the transmitted signal is a linear combination of N sinusoidal carriers, and its baseband equivalent representation in one symbol interval is simply:

$$s_{base}(t) = \sum_{n=-N/2}^{N/2} c_n \cos(2\pi nt/T_s + \theta_n) \ , \ 0 \leq t \leq T_s. \tag{4.1}$$

where f_0 and θ_n are the fundamental frequency and the phase corresponding to the nth channel respectively. Not only do we need to consider the effect of frequency and time variations in chapter 3, but we also need to consider the *phase jitters* (*offsets*) and the *amplitude variations*, which are generally referred as signal distortion.

The *distortionless* or *linear distorted* transmission incurred only if the output signal is a scaled version of the delayed input signal. However, this type of distortion is rarely observed in practice and non-linear distortion should be considered. For a given MC-CDMA signal, the phase distortion can be possibly remedied by the use of synchronization devices such as: phase locked loop and DSP-based synchronizer [26]. Therefore, *amplitude variation* would be our major concern in designing the MC-CDMA signals. The basic measure of *amplitude variation* of a given signal $s(t)$ is the *peak-to-average* ratio or sometimes called: *crest* or *peak* factor; and we will give details on the crest factor of the MC-CDMA signals in the following sections.

4.1 Existence of Signal Distortion

In a communication system, signal distortion is known to be existed in the rear-end of the transmitter or simply *transmission filter* before the signal enters the channel. The transmission filter is used mainly for amplification and channel matching. Two commonly deployed amplifiers used in radio communication systems are:

(i) Traveling Wave Tube Amplifier (TWTA),

(ii) Solid-State Power Amplifier (SSPA).

The TWTA is mostly used in the early days satellite communications. Although it is possible to implement a TWTA by adjusting the interaction between *radio wave* and *electron beam* [27]. However its bulk size; heavy weight; together with its high susceptibility to phase jitters and non-linearity make TWTA not a suitable device installed in the handset, i.e. reverse (upward) link in mobile communication environment.

The SSPA, on the other hand offers significant advantage over TWTA on both the linearity and reliability, hence the transponder capacity [27]. The commonly available solid-state device used at microwave frequencies is the field-effect transistor (FET), which is a unipolar device manipulated by electric current. Gallium Arsenide (GaAs) is the basic material used in nowadays FET fabrication because of its high electron mobility, which resulted in [28]:

(i) Small parasitic resistance,

(ii) Large transconductance,

(iii) Short transit time of electrons.

The above characteristics lead to the desired properties for a power amplifier to operate in microwave frequencies, which are: low noise figure, high gain and cutoff frequencies. Although FET-based SSPA has certain advantages discussed above, yet it is still worthwhile to note the types of signal distortion within itself, they are: cross-modulation and intermodulation [28].

It is interesting to note that the two types of signal distortion stated above are resulted from the *amplitude nonlinearity*, where we assume that the *phase nonlinearity* is

not significant enough to affect the resultant signal. Hence, only small intermodulation products are generated by the fluctuations of carrier phase modulation (i.e. AM-PM conversion). The amplitude nonlinearity is a direct result of the nonlinear transfer characteristic of the transmission amplifier, where the output v_o of a non-linear amplifier can be described by a power series of an input signal v_i as [28]:

$$v_o = k_1 v_i + k_2 v_i^2 + k_3 v_i^3 + \cdots, \tag{4.2}$$

where the k_i's are the coefficients of the ith order of the input signal.

Recently, different types of linear modulation method are proposed [29]: Adaptive Baseband Predistortion and Cartesian Loop Feedback to class C amplifiers, which attain higher efficiency of linear amplification than the conventional class A amplifiers for single carrier communication systems. However for multicarrier systems, especially in cellular basestations, satellite transponders and mobile handsets, where the transmitted signals consist of a simultaneous concatenation of a set of channel information, from which the resultant signals may have a non-uniform envelope. Although different types of hybrid techniques using feedforward and feedback linearization are proposed and claimed to have significant improvement on the amplification range [29], it is yet important to have a desirable control on the transmitted signal envelope so as to minimize the possible variations and hence the irreducible error rate of the system.

4.2 Measures of the Signal Envelope Fluctuation

To put in other words, the problem is to design the transmitted waveform so that its *crest factor* is minimum with a designated spectrum. The crest factor, sometimes called *peak factor* of a given signal is defined to be its peak-to-average ratio. Consider a signal $s(t)$, its *crest factor* (CF) [30] is defined as:

$$CF(s) = \frac{\|s\|_\infty}{\|s\|_2}, \tag{4.3}$$

where $\|s\|_\infty$ (the $\mathbf{L}^\infty$-norm) and $\|s\|_2$ (the $\mathbf{L}^2$-norm) of our system are:

$$\|s\|_\infty = \sup_t |s(t)| = \sup_{|t| \le T_s/2} |w(t)|, \tag{4.4}$$

and

$$\|s\|_2 = \lim_{T\to\infty}\left[\frac{1}{T}\int_{-T/2}^{T/2}|s(t)|^2dt\right]^{1/2} = \left[\frac{1}{T_s}\int_{-T_s/2}^{T_s/2}|w(t)|^2dt\right]^{1/2}. \tag{4.5}$$

respectively. Intuitively, if the crest factor of a signal is large, there must have some irregularities or even glitches appeared as a function of time resulted in unpredictable nonlinear distortions and detection errors. On the other hand, signals with low crest factors can effectively contribute to a wide radiation in transmission or receiving directivity pattern [31]. As discussed in [32, 33], one of the possible ways to design a given signal waveform is by means of the *phase angles* of its Fourier coefficients.

The basic framework of signal design is to use exhaustive search for low-crest waveforms, hence the corresponding sets of phase angles which constitute them. Schroeder and Vyssotsky [31] developed an iterative relationship among the phase angles for a signal with little variations on its envelope. For multitone systems, the construction of a particular phase pattern of the signal spectrum is in fact corresponding to the signature sequences design; while this problem is originated from RADAR applications. Shapiro-Rudin (SR) sequences is a suitable candidates that can be used for the construction of low-crest multitone signals using a systematic recursive algorithm. The basis of Shapiro-Rudin sequences is a pair of polynomials:

$$\begin{cases} p_{n+1}(t) &= p_n(t) + e^{j2^n t}q_n(t) \\ p_{n+1}(t) &= p_n(t) - e^{j2^n t}q_n(t) \end{cases}. \tag{4.6}$$

where $p_0(t) = q_0(t) = 1$. The Fourier transform of both $p_n(t)$ and $q_n(t)$ consists of 2^n frequency components of equal magnitude [31]. Using the substitution $z = e^{jt}$, the first few polynomials are:

$$\begin{cases} p_1 &= 1+z, \quad q_1 = 1-z, \\ p_2 &= 1+z+z^2-z^3, \quad q_2 = 1+z-z^2+z^3, \\ p_3 &= 1+z+z^2-z^3+z^4+z^5-z^6+z^7, \\ p_4 &= 1+z+z^2-z^3-z^4-z^5+z^6-z^7. \end{cases} \tag{4.7}$$

We will showed that the crest factors of the Shapiro-Rudin polynomials are limited to 2, which are in common to those of the sinusoids. Although the value of 2 in the crest

factor is not optimal in terms of amplitude variations, it is good enough to have the power amplifier to operate at the linear region with insignificant system nonlinearity.

Shapiro-Rudin (SR) sequences is a subclass of Golay complementary sequences which can be constructed recursively using the coefficients of the polynomials in (4.7) [30, 34, 31]. In other words, if we have a *basis* or *seed* $\{\alpha,\ \beta\}$, the possible sequences can be constructed would be in the set $\{++, +-, -+, --\}$, ('+'$= +1$, '$-$'$= -1$). The recursive construction is illustrated in Figure 4.1, where we use the notation $x' = -x$. For each iteration, the appended sequence is constructed from the last sequences with duplicate of the first half and inversion of the second half.

$\alpha\beta$

$\alpha\beta\alpha\beta'$

$\alpha\beta\alpha\beta'\alpha\beta\alpha'\beta$

$\alpha\beta\alpha\beta'\alpha\beta\alpha'\beta\alpha\beta\alpha\beta'\alpha'\beta'\alpha\beta'$

Figure 4.1: Construction of SR sequence with seed $\{\alpha,\ \beta\}$.

Boyd justified the importance of signature sequence in the resultant envelope fluctuation of the multitone signals. He showed that if random sequences or m-sequences were used as the spreading code $\{c_n\}_1^N$, the crest factor of the resultant multitone signals can grow unbounded ($\sim \sqrt{\log N}$) as N increases [30]. According to the IS-95 used for the commercially available CDMA system, subsequences of m-sequences are used as the subscribers' signatures in order to spread the desired signal spectrum near the noise floor before transmission. We therefore make a comparison of the multitone signals, one constructed using a subsequence of a given m-sequence, and the other using a SR sequence and evaluate their respective crest factors. In Figure 4.2, multitone signals generated both from the subsequence of a long m-sequence (with 18 stages) and that of SR sequence with length $N = 512$ are shown. The crest factor of the latter was found to be 3.5dB lowered than that of the former on average.

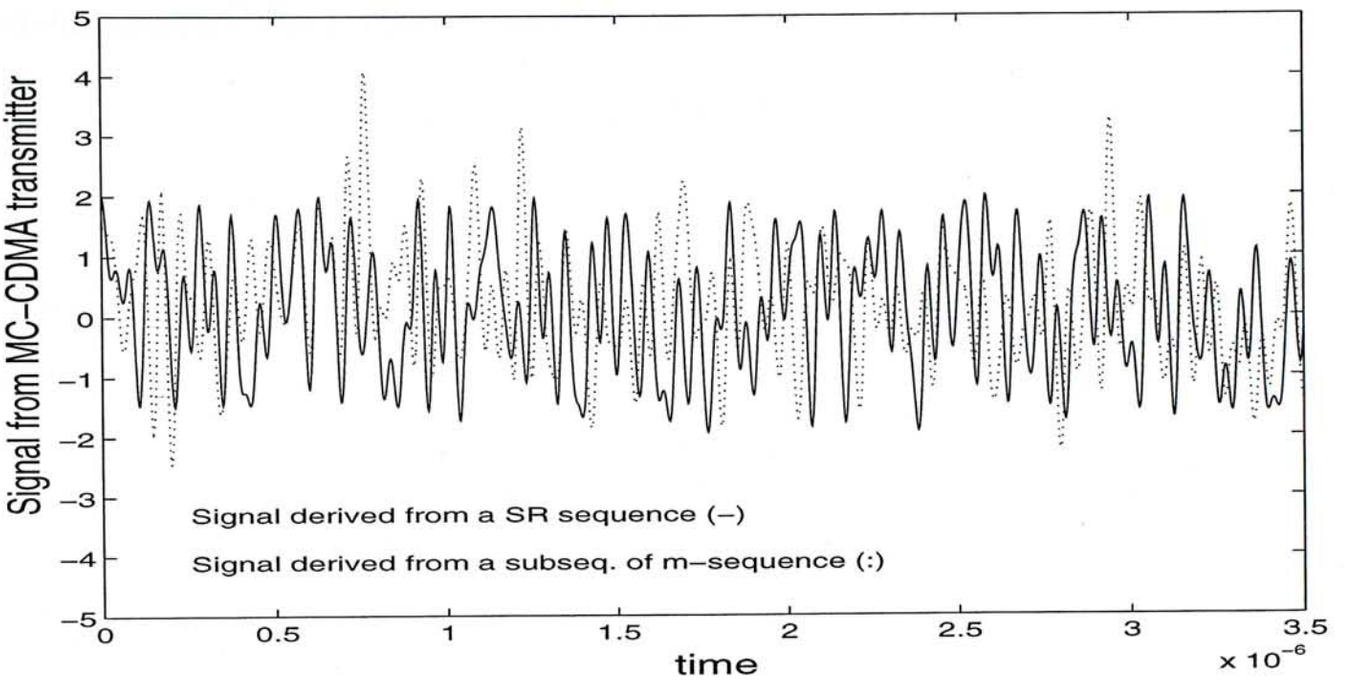

Figure 4.2: Comparison of MC signals constructed from two different signature sequences.

4.3 Complementary Sequences

Study found that complementary sequences are the possible candidates for the purpose of synthesizing low crest multitone waveforms [30]. A pair of sequences $(\{p_n\}, \{q_n\})$, each of length N is called a *Golay complementary pair* if

$$\sum_{n=1}^{N-i} p_n p_{n+i} + \sum_{n=1}^{N-i} q_n q_{n+i} = \begin{cases} 2N & , \quad i = 0 \\ 0 & , \quad otherwise \end{cases} . \tag{4.8}$$

Either member of a complementary pair is a (Golay) *complementary sequence.* The following theorem shows that the crest factor of a MC-CDMA pulse waveform constructed by using a Golay complementary sequence as the signature sequence is upper bounded by 2 (i.e. 6 dB). We focus on the crest factor of the pulse shape.

Theorem 4.1 Let $w(t) = \sum_{n=1}^{N} c_n \cos(\frac{2\pi nt}{T_s})\text{rect}(\frac{t}{T_s})$. If $\{c_n\}_1^N$ is a complementary sequence, then $CF(w) \leq 2$.

Proof: Following similar approach in [34], let $\{c_n\}$ and $\{d_n\}$ form a complementary pair, each with length N [35]. Let $u(t) = \sum_{n=1}^{N} d_n \cos(2\pi nt/T_s)$. Either member of a

complementary pair is called a complementary sequence. Then,

$$\begin{aligned} |w(t)|^2 &\leq |w(t)|^2 + |u(t)|^2, \\ &= \sum_{n=1}^{N} c_n c_n + \sum_{n=1}^{N} d_n d_n = 2N. \end{aligned} \tag{4.9}$$

The first equality in (4.9) holds by the Autocorrelation Theorem in Fourier Transform and we have,

$$CF(w) \leq \frac{\sqrt{2N}}{\sqrt{N/2}} = 2 \quad (6\text{dB}). \tag{4.10}$$

Q.E.D.

There are many construction methods for Golay complementary sequences. The *recursive* method can be described by a 2×2 DFT matrix $\begin{pmatrix} 1 & 1 \\ 1 & -1 \end{pmatrix}$. For a given complementary pair (A, B) of length N, we can then use the DFT matrix to recursively construct other complementary pair $(A^{(1)}, B^{(1)})$ with length $2N$ as follows [36]:

$$\begin{bmatrix} A^{(1)} \\ B^{(1)} \end{bmatrix} = \left[\left(A \times \begin{bmatrix} 1 \\ 1 \end{bmatrix} \right) \left(B \times \begin{bmatrix} 1 \\ -1 \end{bmatrix} \right) \right]. \tag{4.11}$$

In general, polyphase complementary sequences can be constructed using any $M \times N$ matrices with orthogonal columns, which form the basis of the complementary sets of sequences [37]. However, the 6dB bound on the crest factor of the MC-CDMA signals restricted us to focus on the complementary (binary or polyphase) pairs rather than the triads, quads and any other set of sequences.

4.4 Crest Factors

We study the effect of filtering on the crest factors of MC-CDMA signals with Golay complementary sequences as signature sequences and DS-CDMA signals with PN sequences as signature sequences. Derivation is given for three filters: the time-limited pulses, band-limited pulses and raised-cosine shaped pulses.

4.4.1 Time-limited Pulse

4.4.1.1 DS-CDMA

The time-limited baseband transmitted signal consists of rectangular waveforms (chips) oscillating between +1 and −1. The transmitted signal waveform is

$$w(t) = \sum_{n=1}^{N} c_n \text{rect}(\frac{t - nT_c}{T_c}), \tag{4.12}$$

where $\{c_n\}$ is a PN sequence and $T_c = T_s/N$ is the chip duration. It is easily to observe that the peak-to-average ratio of its crest factor equals 1 (0dB).

4.4.1.2 MC-CDMA

The transmitted signal waveform is

$$w(t) = \sum_{n=1}^{N} c_n \cos(\frac{2\pi nt}{T_s})\text{rect}(\frac{t - T_s/2}{T_s}). \tag{4.13}$$

The crest factor is shown to be upper bounded by 6dB in Theorem 1, provided its signature sequence $\{c_n\}$ is a complementary sequence.

4.4.2 Ideally Band-Limited Pulses

4.4.2.1 DS-CDMA

The ideally band-limited pulse shape is

$$w(t) = \sum_{n=1}^{N} c_n \text{sinc}(\frac{Nt - nT_s}{T_s}). \tag{4.14}$$

Assume $\{c_n\}_1^N$ is a PN sequence, $N = 2^e - 1$, e is an even integer. Then there exist i such that

$$\begin{aligned} (c_i, c_{i+1}, ..., c_{i+e/2-1}) &= (c_{i-1}, c_{i-2}, ..., c_{i-e/2}), \\ &= (+1, -1, +1, -1, ..., (-1)^{e/2-1}). \end{aligned} \tag{4.15}$$

Then

$$w\left(\frac{(i-1/2)T_s}{N}\right) = 2\sum_{n=1}^{e/2} |\text{sinc}(n - \frac{1}{2})| + \sum_{\substack{|n-1/2|>e/2 \\ 1\le n-i+1/2\le N}} c_n \text{sinc}(n - \frac{1}{2}),$$

$$= 2\sum_{n=1}^{e/2} \frac{1}{n-1/2} + \sum_{\substack{|n-1/2|>e/2 \\ 1\le n+i-1\le N}} c_n \mathrm{sinc}(n-\frac{1}{2}). \tag{4.16}$$

The first expression grows in the order of $\log N$. (All logaritms in this paper are of base 2.) It is unbounded as N grows to infinity. The second expression corresponds to other terms of smaller magnitude. If we assume the coefficients are random, then the expected value of the second expression is zero. Therefore, the crest factor of ideally band-limited DS-CDMA pulse is likely to grow without bound ($\sim \log\log N$) if the spreading code $\{c_n\}$ is a PN sequence. The theoretical estimate and the experimental data of the crest factor against the number of chips used are shown in Figure 4.3. The solid line is the moving window average of the experimental data obtained on every 21 sample-frame.

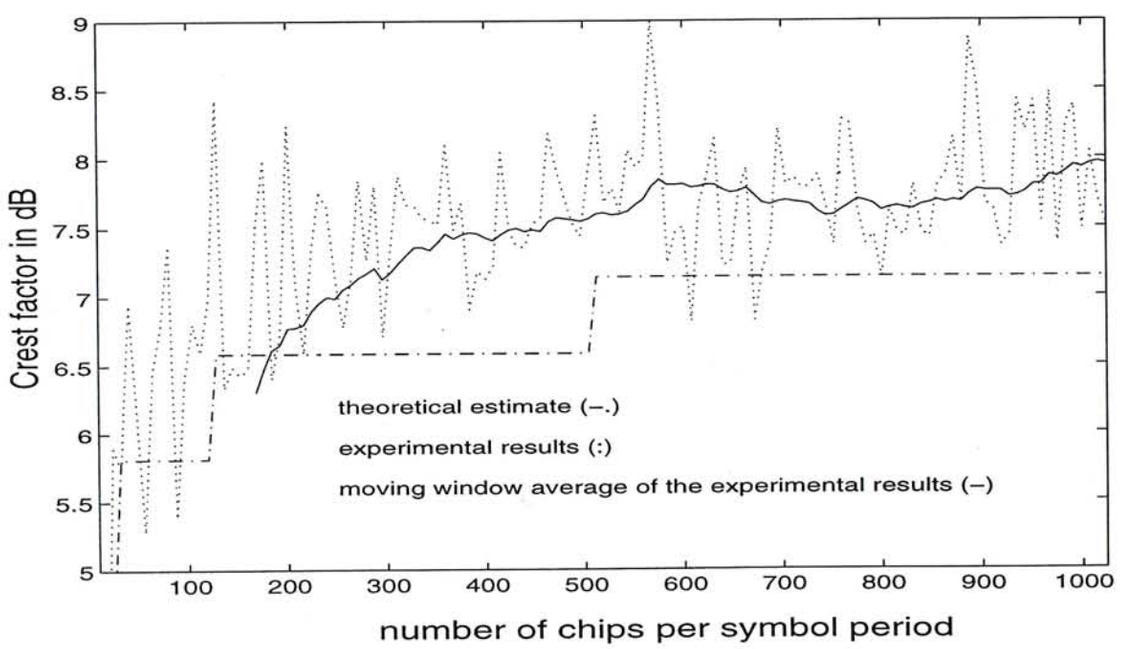

Figure 4.3: Signal performance in DS-CDMA system (sinc chips).

4.4.2.2 MC-CDMA

The pulse shape is

$$w(t) = p(t)h(t),$$

where $p(t) = \sum_{n=1}^{N} c_n \cos(2\pi nt/T_s)$, and $h(t) = \mathrm{sinc}(t/T_s)$. If $\{c_n\}$ is a complementary sequence, then its crest factor of $w(t)$ is bounded by 6 dB because

$$\sup_t w(t) \le (\sup_t p(t)) \cdot (\sup_t h(t)) \le \sqrt{2N} \cdot 1, \tag{4.17}$$

and

$$\int_{-\infty}^{\infty} |w(t)|^2 dt = \int_{-\infty}^{\infty} |W(f)|^2 df = (1/2) \cdot N. \tag{4.18}$$

4.4.3 Shaped Pulses

4.4.3.1 DS-CDMA

With raised-cosine chip shaping, the pulse is

$$w(t) = \sum_{n=1}^{N} c_n \mathrm{rcos}(\frac{Nt}{T_s} - n), \tag{4.19}$$

where

$$\mathrm{rcos}(x) = \mathrm{sinc}(x) \left[\frac{\cos(\pi r x)}{1 - (2rx)^2} \right]. \tag{4.20}$$

Assume c_n is a PN sequence, $N = 2^e - 1$, e is an even integer. Then there exists i and special bit pattern $(c_{i-e/2}, c_{i-e/2+1}, \ldots, c_{i+e/2-1}) = (+1, -1, +1, -1, \cdots)$ or $(-1, +1, -1, +1, \cdots)$ such that

$$w\left(\frac{(i - \frac{1}{2})T_s}{N}\right) = 2\sum_{n=1}^{e/2} |\mathrm{rcos}(n - \frac{1}{2})| + \sum_{\text{other } n} c_n \mathrm{rcos}(n - \frac{1}{2}). \tag{4.21}$$

The first expression is bounded as N grows to infinity; but the bound is larger for smaller r. Note that the raised cosine function equals the sinc function when $r = 0$. The expected value of the second expression is zero, provided the coefficients c_n, for "other" n, are random. The characteristics of the pulse envelope using the raised-cosine filter are shown in Figure 4.4 and Figure 4.5. It remains an open problem to determine whether the asymptotic crest factor is bounded.

4.4.3.2 MC-CDMA

We consider raised-cosine shaping with $r < 1$ only. We switch to complex notations temporarily for the following theorem.

Theorem 4.2 Let $\{c_n\}$ and $\{d_n\}$ be a complementary sequence pair. Let

$$p(t) = \sum_{n=1}^{N} c_n e^{j2\pi nt/T_s},$$

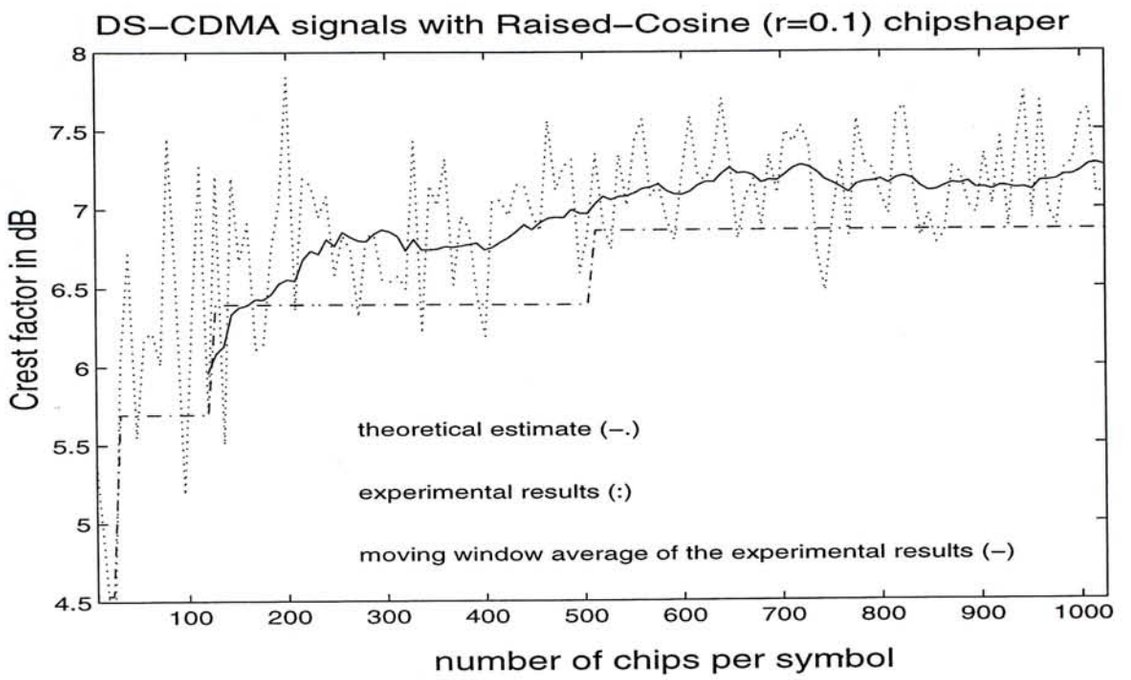

Figure 4.4: Signal performance in DS-CDMA system (raised-cosine chips).

$$\begin{aligned} q(t) &= \sum_{n=1}^{N} d_n e^{j2\pi nt/T_s}, \\ w(t) &= p(t)h(t), \\ v(t) &= q(t)h(t), \\ h(t) &= \mathrm{sinc}(\frac{t}{T_s})[\frac{\cos(\pi rt/T_s)}{1-(2rt/T_s)^2}]. \end{aligned}$$

Assume $r < 1$. Then

$$\min\{CF(w); CF(v)\} \leq \sqrt{2}. \tag{4.22}$$

Proof: Let $(\{c_n\}, \{d_n\})$ be a complementary pair, $v(t) = q(t)h(t)$ and

$$\begin{aligned} q(t) &= \Re\{\sum_{n=1}^{N} d_n e^{j2\pi nt/T_s}\}, \\ P(f) &= \sum c_n \delta(f - n/T_s), \\ Q(f) &= \sum d_n \delta(f - n/T_s), \\ W(f) &= \sum c_n H(f - n/T_s), \\ V(f) &= \sum d_n H(f - n/T_s). \end{aligned}$$

The autocorrelation of $W(f)$ is

$$\int W(f)W^*(f+x)df = \sum_n \sum_m c_n c_m^* \int H(f - n/T_s)H^*(f + x - m/T_s)df$$

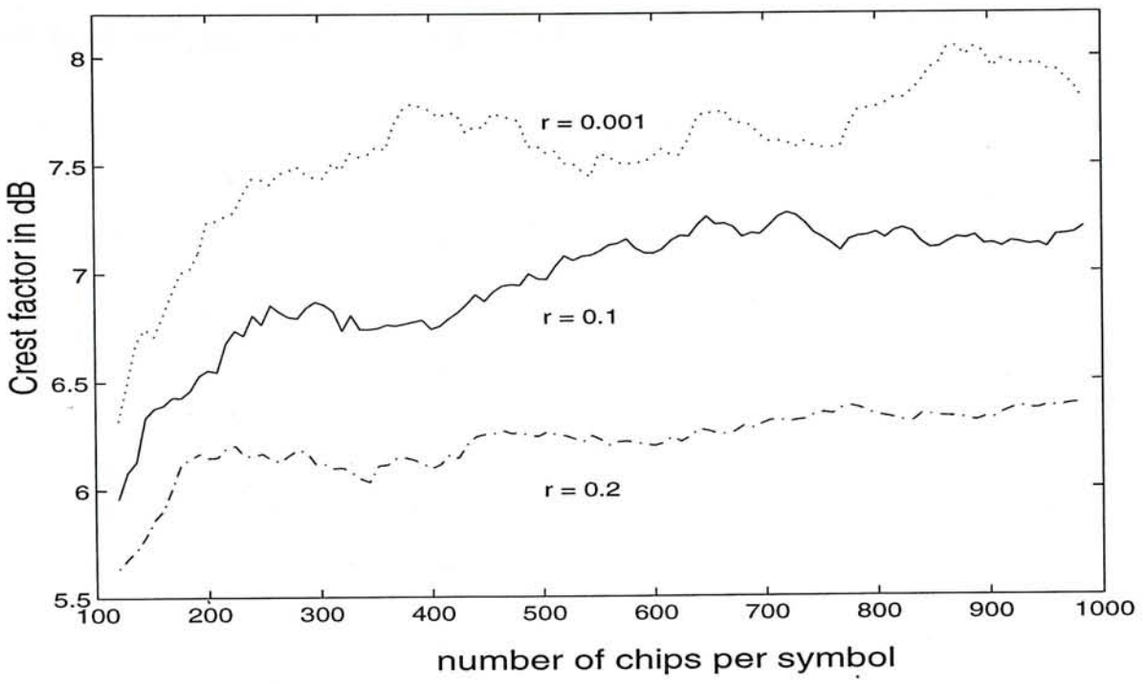

Figure 4.5: Performance of DS-CDMA system using different raised-cosine filters.

$$= \sum_{\ell}(\sum_{n} c_n c^*_{n-\ell}) \int H(f)H^*(f+x-\ell/T_s)df. \tag{4.23}$$

Similarly,

$$\int V(f)V^*(f+x)df = \sum_{\ell}(\sum_{n} d_n d^*_{n-\ell}) \int H(f)H^*(f+x-\ell/T_s)df. \tag{4.24}$$

Therefore,

$$\int W(f)W^*(f+x)df + \int V(f)V^*(f+x)df = 2N \int H(f)H^*(f+x)df. \tag{4.25}$$

Taking the Fourier transform of both sides (via the Autocorrelation Theorem) and setting $x = 0$, we obtain

$$\sup_t |w(t)|^2 \leq 2N \sup_t |h(t)|^2, \tag{4.26}$$

for all t.

Remark: A common shaping is the raised cosine

$$h(t) = \text{sinc}(\frac{t}{T_s}) \left[\frac{\cos(\pi r t/T_s)}{1-(2rt/T_s)^2} \right]. \tag{4.27}$$

The $\mathbf{L^2}$-norm satisfies

$$\int |W(f)|^2 df = (\sum_{n} c_n^2) \int |H(f)|^2 df + 2\Re \left\{ (\sum_{n} c_n c^*_{n-1}) \int H(f)H^*(f-\frac{1}{T_s})df \right\},$$

$$\int |V(f)|^2 df = (\sum_{n} d_n^2) \int |H(f)|^2 df + 2\Re \left\{ (\sum_{n} d_n d^*_{n-1}) \int H(f)H^*(f-\frac{1}{T_s})df \right\}.$$

Because $\{c_n\}$ and $\{d_n\}$ are complementary,

$$\sum_n c_n c_{n-1}^* + \sum_n d_n d_{n-1}^* = 0.$$

Therefore, one of the two terms above is non-negative and at least one of $CF(w)$ and $CF(v)$ is upper bounded by $\sqrt{2}$.

Q.E.D.

If we use real-valued pulses, then the crest factor is upper bounded by 6 dB, as shown in the following Corollary.

Corollary 4.1 In the theorem above,

$$\min\{CF(\Re\{p(t)\}; CF(\Re\{q(t)\})\} \leq 2. \tag{4.28}$$

4.5 Spectrally Efficient Complementary (SEC) Sequences

In this section, we consider non-filtered pulse waveforms and consider its spectral roll-off. We find that certain subsets of complemetary sequences result in MC-CDMA pulse waveforms whose power spectrum outside the main lobe decreases faster than otherwise.

Let $w(t)$ denote the MC-CDMA pulse waveform, and let $W(f)$ denote its Fourier transform. Then the power spectral density of signal waveform $s(t)$ is given by $\mathcal{P}_s(f) = \frac{1}{T_s}|W(f)|^2$. A complementary sequence $\{c_n\}$ is called a **spectrally efficient complementary (SEC) sequence** if $\sum_{n=1}^{N}(-1)^n c_n = 0$.

Theorem 4.3 Let $s(t)$ and $w(t)$ be the same as shown in section II. Assume $\{c_n\}$ is a complementary sequence. Let $\mathcal{P}_s(f)$ denote the power spectral density of $s(t)$. Then, for large $|f|$,

$$\begin{cases} |\mathcal{P}_s(f)| & \propto & 1/f^4, \text{ if } \{c_n\} \text{ is a SEC sequence} \\ |\mathcal{P}_s(f)| & \propto & 1/f^2, \text{ otherwise} \end{cases}$$

Proof: The power spectral density of the signal $s(t)$ is

$$\begin{aligned}
\mathcal{P}_s(f) &= \frac{1}{T_s}|W(f)|^2, \\
&= T_s\left|\sum_{n=1}^{N} c_n \frac{\sin[\pi(f-n/T_s)T_s]}{\pi(f-n/T_s)T_s}\right|^2, \\
&= T_s\left|\sum_{n=1}^{N} \frac{(-1)^n c_n \sin \pi f T_s}{\pi T_s(f-n/T_s)}\right|^2, \\
&= \frac{1}{\pi^2 T_s}\left|\sum_{n=1}^{N}(-1)^n c_n\left(\frac{\sin \pi f T_s}{f-n/T_s}\right)\right|^2, \\
&= \frac{\sin^2(\pi f T_s)}{\pi^2 T_s}\left|\sum_{n=1}^{N}\frac{(-1)^n c_n}{f-n/T_s}\right|^2, \\
&= \frac{\sin^2(\pi f T_s)}{\pi^2 T_s}\left[-\frac{c_1}{f-1/T_s}+\frac{c_2}{f-2/T_s}-\cdots+(-1)^N\frac{c_N}{f-N/T_s}\right]^2, \\
&= \frac{\sin^2(\pi f T_s)}{\pi^2 T_s}\left[\frac{\sum_{n=1}^{N}(-1)^n c_n f^{N-1}+G(f)}{(f-1/T_s)(f-2/T_s)\cdots(f-N/T_s)}\right]^2. \qquad (4.29)
\end{aligned}$$

where $G(f)$ is a polynomial in f of degree $N-2$. (i.e. $G(f) = \mathcal{G}f^{N-2}+\cdots$, where $\mathcal{G} = \sum_{n=1}^{N}\sum_{\substack{m=1\\ \neq n}}^{N}(-1)^{n+1}mc_n/T_s)$. If the term $\sum_{n=1}^{N}(-1)^n c_n$ vanishes, we have:

$$\mathcal{P}_s(f) = \frac{\mathcal{G}^2\sin^2(\pi f T_s)}{\pi^2 T_s}\left[\frac{f^{N-2}+\cdots}{f^N+\cdots}\right]^2. \qquad (4.30)$$

As $f \gg N/T_s$, we have

$$\begin{aligned}
\mathcal{P}_s(f) &\approx \frac{\mathcal{G}^2\sin^2(\pi f T_s)}{\pi^2 T_s}\left(\frac{f^{N-2}}{f^N}\right)^2, \\
&\propto \frac{1}{f^4}. \text{ (when } f \gg N/T_s.) \qquad (4.31)
\end{aligned}$$

If $\sum_{n=1}^{N}(-1)^n c_n \neq 0$, then $|W(f)|^2$ is roughly in proportion to $1/f^2$.

Q.E.D.

Example (Figure 4.6): A broadband (~50MHz) MC-CDMA system is chosen for demonstration by using the baseband model described in section 2.3.3. Signals derived from a non-spectrally efficient complementary sequence and a SEC sequence are compared in both time and frequency domain. The data sequence is randomly generated, while the non-SEC sequence and the SEC sequence are chosen to be $\{-\ -\ +\ -\ +\ -\ -\ -\}$ and $\{-\ -\ +\ -\ -\ +\ +\ +\}$ respectively. Notice the sharper roll-off gradient of the spectrum is in the dotted line.

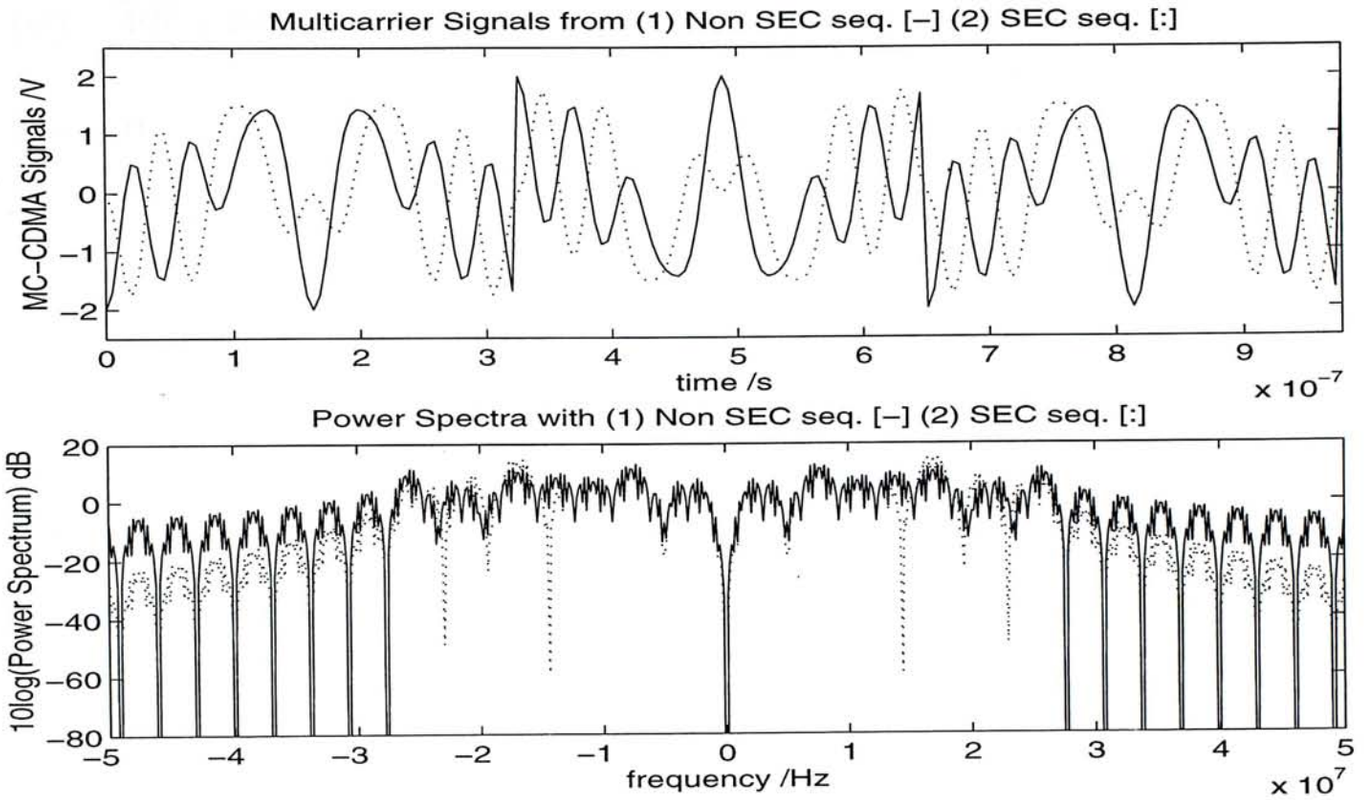

Figure 4.6: Comparison of the spectral efficiency from two MC-CDMA signals.

4.6 Construction of Spectrally Efficient Complementary (SEC) Sequences

We study methods of constructing SEC sequences. Given a SEC sequence, a lot more of its counterparts can be generated. In the following synthesis, we let $A = \{a_1,\ a_2,\ \ldots,\ a_N\}$ and $B = \{b_1,\ b_2,\ \ldots,\ b_N\}$.

Theorem 4.4 Let (A, B) be a complementary pair where either of the sequences has even length N, and let AB be a SEC sequence. Then the following sequences of length $2N$ are also SEC sequences:

(i) BA (interchanging the way of concatenation),

(ii) $A'B'$ (altering both the concatenated pair),

(iii) $\tilde{A}\tilde{B}$ (reversing both the concatenated pair),

(iv) $\tilde{A}B', A'\tilde{B}$ (reversing either one of the series and altering the other),

(v) $\widetilde{A'}B, A\widetilde{B'}$ (altering and reversing either one of the series),

(vi) $\widetilde{A'}\widetilde{B'}$ (altering and reversing both series).

Proof: By the 5th property of [35], all these sequences are complementary sequences. Since AB is a SEC sequence, we have

$$\sum_{n=1}^{N}[(-1)^n a_n + (-1)^{N+n} b_n] = 0, \tag{4.32}$$

$$\Rightarrow \sum_{n=1}^{N}[(-1)^n a_n + (-1)^n b_n] = 0. \quad (N \text{ is even}) \tag{4.33}$$

It is easy to see that (i) and (ii) in Theorem 4.4 are true. Let $\mu = \sum_{n=1}^{N}(-1)^n a_n$, then

$$\begin{aligned} \nu = \sum_{n=1}^{N}(-1)^n \tilde{a}_n &= \sum_{n=1}^{N}(-1)^n a_{N-(n-1)}, \\ &= \sum_{m=N}^{1}(-1)^{N-m+1} a_m, \\ &= -\sum_{m=1}^{N}(-1)^m a_m = -\mu. \end{aligned} \tag{4.34}$$

Then (iii) to (vi) in Theorem 4.4 becomes trivial.

Q.E.D.

Example: Let $A = \{- \ - \ + \ -\}$ and $B = \{- \ - \ - \ +\}$, we have $AB = \{- \ - \ + \ - \ - \ - \ - \ +\}$ as a SEC sequence. Then, we can construct fifteen other SEC sequences by the six operations in Theorem 4.4 as follows:

(a) $BA = \{- \ - \ - \ + \ - \ - \ + \ -\}$

(b) $A'B' = \{+ \ + \ - \ + \ + \ + \ + \ -\}$

(c) $B'A' = \{+ \ + \ + \ - \ + \ + \ - \ +\}$

(d) $\tilde{A}\tilde{B} = \{- \ + \ - \ - \ + \ - \ - \ -\}$

(e) $\tilde{B}\tilde{A} = \{+ \ - \ - \ - \ - \ + \ - \ -\}$

(f) $\tilde{A}B' = \{- \ + \ - \ - \ + \ + \ + \ -\}$

(g) $\tilde{B}A' = \{+ \ - \ - \ - \ + \ + \ - \ +\}$

(h) $A'\tilde{B} = \{+ \ + \ - \ + \ + \ - \ - \ -\}$

(i) $B'\tilde{A} = \{+ \ + \ + \ - \ - \ + \ - \ -\}$

(j) $\widetilde{A'}B = \{+ \ - \ + \ + \ - \ - \ - \ +\}$

(k) $\widetilde{B'}A = \{- \ + \ + \ + \ - \ - \ + \ -\}$

(l) $A\widetilde{B'} = \{- \ - \ + \ - \ - \ + \ + \ +\}$

(m) $B\widetilde{A'} = \{- \ - \ - \ + \ + \ - \ + \ +\}$

(n) $\widetilde{A'}\widetilde{B'} = \{+ \ - \ + \ + \ - \ + \ + \ +\}$

(o) $\widetilde{B'}\widetilde{A'} = \{- \ + \ + \ + \ + \ - \ + \ +\}$

Theorem 4.5 (Iterative construction) If (A, B) is a complementary pair and A is a SEC sequence, then $(ABAB', ABA'B)$ is a complementary pair and $ABAB'$ is a SEC sequence.

Proof: Using the 9th property in [35] recursively, we obtain the complementary pair $(ABAB', ABA'B)$ from the complementary pair (A, B). As $\sum_{n=1}^{N}(-1)^n a_n = 0$ and by definition, $\sum_{n=1}^{N}(-1)^n b_n = -\sum_{n=1}^{N}(-1)^n b'_n$, hence $ABAB'$ is a SEC sequence.

Q.E.D.

Theorem 4.6 If (A, B) be a complementary pair (each of length N), and

$$\sum_{n=1}^{N}(-1)^n a_n = \sum_{n=1}^{N}(-1)^n b_n.$$

Then (AB, AB') is complementary and at least one of the pair is spectrally efficient.

Proof: From [35], (AB, AB') is a complementary pair given that A and B are complementary. Then assuming $\sum_{n=1}^{N}(-1)^n a_n = \mu$, α and β be $[\sum_{n=1}^{N}(-1)^n a_n + \sum_{n=1}^{N}(-1)^n b_n]$ and $[\sum_{n=1}^{N}(-1)^n a_n + \sum_{n=1}^{N}(-1)^n b'_n]$ respectively, then we have

Case 1: $\mu \neq 0$.

$$\begin{aligned} \alpha &= \sum_{n=1}^{N}(-1)^n a_n + \sum_{n=1}^{N}(-1)^n b_n \quad (N \text{ is even}), \\ &= 2\mu \neq 0. \end{aligned} \tag{4.35}$$

Case 2: $\mu = 0$, and $\alpha = 0$ by definition.
In both cases, $\beta = \sum_{n=1}^{N}(-1)^n a_n - \sum_{n=1}^{N}(-1)^n b_n$. As the $\sum_{n=1}^{N}(-1)^n a_n$ equals $\sum_{n=1}^{N}(-1)^n b_n$, therefore $\beta = 0$.

Q.E.D.

Theorem 4.7 If (A, B) is a complementary pair and A is a SEC sequence of length N. Then $2N$ is the square of an integer.

Proof: According to the property 5f) in [35], $(\widehat{A}, \widehat{B})$ is also a complementary pair, where $\widehat{X}$ is the sequence obtained from altering the elements in x of even order. Let p and q be the number of '$-$' in $\widehat{A}$ and $\widehat{B}$ respectively. We have

$$\sum_{n=1}^{N} \widehat{a}_n = \sum_{n=1}^{N} (-1)^n a_n = 0. \tag{4.36}$$

Therefore, $\widehat{A}$ contains $N/2$ $+$'s and $N/2$ $-$'s. The 8th property of [35] states that

$$N = (N - p - q)^2 + (p - q)^2, \tag{4.37}$$

where p is the number of $-$'s in A and q is the number of $-$'s in B. Setting $p = \frac{N}{2}$, we have

$$N = 2(\frac{N}{2} - q)^2 \quad \text{or} \quad q = \frac{1}{2}(N \mp \sqrt{2N}). \tag{4.38}$$

Therefore, $\sqrt{2N}$ must be an integer.

Q.E.D.

Therefore, the length of SEC sequences must be 2, 8, 18, 32, 50, 72, 98, 128, ..., $(1/2)i^2$, ..., etc. Our methods exhibit SEC sequences of length 2, 8, 32, 128, already. There is no complementary pair of length 18 [35].

Theorem 4.8 If A and B are complementary with each other, and $\sum_{n=1}^{N} a_n = \sum_{n=1}^{N} b_n$, then the sequence formed by interleaved concatenation of A and B (i.e. $\{a_1, b_1, a_2, b_2, \ldots, a_N, b_N\}$) is a SEC sequence.

Proof: According to the 10th property of [35], the interleaved sequences $\{a_1, b_1, a_2, b_2, \ldots, a_N, b_N\}$ and $\{a_1, b'_1, a_2, b'_2, \ldots, a_N, b'_N\}$ form a complementary pair. Furthermore,

$$\sum_{n=1}^{N} (-1)^{2n+1} a_n + \sum_{n=1}^{N} (-1)^{2n} b_n = -\sum_{n=1}^{N} a_n + \sum_{n=1}^{N} b_n = 0. \tag{4.39}$$

Therefore, the sequence formed by interleaved concatenation of a complementary series (A, B) with the condition $\sum_{n=1}^{N} a_n = \sum_{n=1}^{N} b_n$ is a SEC sequence.

Q.E.D.

Example: Let $A = \{- \ - \ + \ -\}$ and $B = \{+ \ - \ - \ -\}$. Then (A, B) is a complementary pair, $\sum_{n=1}^{N} a_n = \sum_{n=1}^{N} b_n$, and their interleaved concatenation, $\{- \ + \ - \ - \ + \ - \ - \ -\}$, is a SEC sequence.

Theorem 4.9 Let $C = c_1, c_2, \ldots, c_m$ and $D = d_1, d_2, \ldots, d_m$ form a complementary pair independent of (A, B). If AB is a SEC sequence and either C or its inverse C' equals $\wp(D)$, then either the sequence

$$U = A^{c_1} \ A^{c_2} \ \cdots \ A^{c_m} B^{d_1} \ B^{d_2} \ \cdots \ B^{d_m}$$

or

$$V = A^{d_m} A^{d_{m-1}} \cdots A^{d_1} \ B^{c_m'} B^{c_{m-1}'} \cdots B^{c_1'}$$

is a SEC sequence of length $2mN$, where $\wp(x)$ is a sequence resulted from any permutation of the elements in x.

Proof: Let $U = \{u_1, u_2, \ldots, u_{2mN}\}$ and $V = \{v_1, v_2, \ldots, v_{2mN}\}$. The complementary relationship between U and V was already proved in [35]. As AB is a SEC sequence, we have $\sum_{n=1}^{N}(-1)^n a_n = -\sum_{n=1}^{N}(-1)^n b_n$. Now, if C can be formed by any permutation of D (i.e. the number of +'s (−'s) in C equals the number of +'s (−'s) in D), we can then select the pair (A^{c_i}, B^{d_j}) such that $c_i = d_j$ for any $i, j \in \{1, \ldots, m\}$. We can then obtain $\sum_{k=1}^{2mN}(-1)^k u_k = 0$. The proof for $\sum_{k=1}^{2mN}(-1)^k v_k = 0$ given $C' = \wp(D)$ can be obtained using the same approach as shown above.

Q.E.D.

Example: Let $C = \{+ \ - \ - \ -\}$ and $D = \{- \ + \ - \ -\}$. We then have $U = \{A, -A, -A, -A, \ -B, B, -B, -B\}$ and $V = \{-A, -A, A, -A, B, B, B, -B\}$. As we can see that $C = \wp(D)$, and by the fact that AB is complementary, $\sum_{k=1}^{2mN}(-1)^k u_k = -2 \cdot (\sum_{n=1}^{N}(-1)^n a_n + \sum_{n=1}^{N}(-1)^n b_n) = 0$. Hence, U is an example of SEC sequence constructed from Theorem 4.9.

Remarks: It is not difficult to realize that either X or Y of the following is a SEC sequence.

$$X = A^{c_1} \ B^{d_1} \ A^{c_2} \ B^{d_2} \ \cdots \ A^{c_m} \ B^{d_m}$$

or $$Y = A^{d_m} B^{c_{m'}} \cdots A^{d_{m-1}} B^{c_{m-1'}} A^{d_m} B^{c_{m'}}$$

It is realized that given two complementary pairs with length m and N respectively, if a concatenation of one set of series is a SEC sequence, other SEC sequences of length $2mN$ can be synthesized.

4.7 Generalized Multiphase Spectrally Efficient Complementary Sequences

The analysis above is restricted to binary sequences ($c_n = \pm 1$). However, the multiphase spectrally efficient complementary (MPSEC) sequences ($c_n = e^{j\Phi_n} = x_n + jy_n$) can be obtained based on multiphase complementary (MPC) pair [38]. A multiphase complementary sequence is a member of a MPC pair and it is found that the criterion for a multiphase complementary sequences to be spectrally efficient in MC-CDMA (signal power decades as $1/f^4$) is $\sum_{n=1}^{N}(-1)^n x_n = \sum_{n=1}^{N}(-1)^n y_n = 0$.

However, the possible lengths of the existing MPSEC sequences are different from the binary SEC sequences illustrated in Theorem 4.7. For simplicity, we derive the situation of quadriphase sequences over the alphabet $\alpha_4 = \{-j, -1, +j, +1\}$ and we obtain a theorem similar to Theorem 4.7 for the SEC sequences over α_4.

Theorem 4.10 Let (P,Q) be a complementary pair over the alphabet $\{-j, -1, +j, +1\}$ of even lengths (N say), and P be a MPSEC sequence with $\sum_{n=1}^{N} p_n = 0$. Then,

$$\begin{aligned} N \;=\; & (\textit{Sum of the square of the presence of any element of } \alpha_4 \textit{ in } Q) \\ & -[(\textit{no. of } `+' \textit{ in } P)^2 + (\textit{no. of } `-' \textit{ in } P)^2]. \end{aligned} \tag{4.40}$$

Proof: Let $P = \{p_1, p_2, \ldots, p_N\}$ and $Q = \{q_1, q_2, \ldots, q_N\}$ be a MPC pair and P is a MPSEC sequence. Hence, we have

$$\sum_{n=1}^{N}(-1)^n p_n = 0. \tag{4.41}$$

We can see that the sum of the elements of the sequence $\widehat{P} = \{(-1)^n p_n\}$ is zero. By the fact that (P, Q) is a MPC pair, $(\widehat{P}, \widehat{Q})$ is also a MPC pair, where $\widehat{Q} = \{(-1)^n q_n\}$. Also, the condition in (4.41) implies that the number of $+1$'s ($+j$'s) equals the number of -1's ($-j$'s) in $\widehat{P}$. By the complementary property, we have:

$$\sum_{n=1}^{N-k} p_n p_{n+k}^* + \sum_{n=1}^{N-k} q_n q_{n+k}^* = \begin{cases} 2N & , \quad k = 0 \\ 0 & , \quad k \neq 0. \end{cases} \tag{4.42}$$

where '*' denotes the complex conjugate. The condition for $k \neq 0$ in (4.42) means that the sum of product of any pairings with a given separation in P equals the inverse of that in Q. We assume further that x be the number of '+1' in $\widehat{P}$, while u, v and w be the number of '+1', '-1' and '$+j$' in $\widehat{Q}$ respectively. In the probabilistic point of view, we have in the *real* domain:

Possible pairings constitute '+1' in P = Possible pairings constitute '-1' in Q (4.43)

As the possible pairings constitute '+1' in P are (+1,+1), (-1,-1), (j,j) and ($-j$,$-j$), while the possible pairings constitute '-1' in Q are (+1,-1), (-1,+1), (j,$-j$) and ($-j$,j). Hence,

$$x(x-1) + (N-2x)\left(\frac{N-2x}{2} - 1\right) = uv + w(N-u-v-w). \tag{4.44}$$

Then, we have the condition of a pair of MPSEC sequences $\{P, Q\}$ as:

$$N = u^2 + v^2 + w^2 + (N-u-v-w)^2 - x^2 - \left(\frac{N-2x}{2}\right)^2. \tag{4.45}$$

Q.E.D.

A program is written to test from length of 2 to 100, and we obtain the possible lengths of MPSEC sequences to be : 2, 4, 8, 10, 16, 18, 20, 26, 32, 34, 36, 40, 50, 52, 58, 64, 68, 72, 74, 80, 82, 90, 98, 100.

It is noted that the theorems derived in section 4.6 for binary SEC sequences are generally true for MPSEC sequences with the modifications that the reverse operation

is accompanied by conjugation and the exponent denote as *phase modulation* of the elements. These modifications can be illustrated in the following examples.

Example 1: The sixteen distinct MPSEC sequences can be obtained when Theorem 4.4 is applied to a MPC pair $P = \{-\ j\ -\ -j\}$ and $Q = \{+\ j\ +\ -j\}$ as follows:

(a) $PQ = \{-\ j\ -\ -j\ +\ j\ +\ -j\}$ (i) $P'\tilde{Q} = \{+\ -j\ +\ j\ +\ -\ -\ -\}$

(b) $QP = \{+\ j\ +\ -j\ -\ j\ -\ -j\}$ (j) $Q'\tilde{P} = \{-\ -j\ -\ j\ j\ -\ -j\ -\}$

(c) $P'Q' = \{+\ -j\ +\ j\ -\ -j\ -\ j\}$ (k) $\widetilde{P'}Q = \{-j\ +\ j\ +\ +\ j\ +\ -j\}$

(d) $Q'P' = \{-\ -j\ -\ j\ +\ -j\ +\ j\}$ (l) $\widetilde{Q'}P = \{-j\ -\ j\ -\ -\ j\ -\ -j\}$

(e) $\tilde{P}\tilde{Q} = \{j\ -\ -j\ -\ j\ +\ -j\ +\}$ (m) $P\widetilde{Q'} = \{-\ j\ -\ -j\ -j\ -\ j\ -\}$

(f) $\tilde{Q}\tilde{P} = \{j\ +\ -j\ +\ j\ -\ -j\ -\}$ (n) $Q\widetilde{P'} = \{+\ j\ +\ -j\ -j\ +\ j\ +\}$

(g) $\tilde{P}Q' = \{j\ -\ -j\ -\ -\ -j\ -\ j\}$ (o) $\widetilde{P'}\widetilde{Q'} = \{-j\ +\ j\ +\ -j\ -\ j\ -\}$

(h) $\tilde{Q}P' = \{j\ +\ -j\ +\ +\ -j\ +\ j\}$ (p) $\widetilde{Q'}\widetilde{P'} = \{-j\ -\ j\ -\ -j\ +\ j\ +\}$

Example 2: In complex domain the exponent of Theorem 4.9 can be interpreted as *phase modulation* to the given sequence's elements. As an example, we consider the pair (P, Q) in Example 1 together with the MPC pair $R = \{-1\ -j\ -1\ j\}$ and $S = \{j\ -1\ -j\ -1\}$. As $R = \wp(S)$, the sequence $U = \{P^{-1}\ P^{-j}\ P^{-1}\ P^{j}\ Q^{j}\ Q^{-1}\ Q^{-j}\ Q^{-1}\}$ is a MPSEC sequence. The sequence U can be obtained by the notification of the transformations: $+1^{j} = j$, $+1^{-j} = -j$, $j^{j} =$ '$-$' and $j^{-j} =$ '$+$'. Note that the 'alternation' in the exponent for the binary SEC sequences can be viewed as a particular case to the concept of *phase modulation.*

Chapter 5

Summary and Future Extensions

5.1 Summary of the Results

The performance analysis of the newly proposed MC-CDMA is compared to the DS-CDMA using Gaussian approximation (G.A.) in the reverse link mobile communications. It is found that the MC-CDMA outperforms DS-CDMA under the assumptions of uniformly distributed random phase and delay; and also identical independent distributed (i.i.d.) data sequence with rectangular pulses without *guard interval.* Like DS-CDMA, the performance of MC-CDMA is dependent on the pulse shape. However, the relationship is quite complicated and cannot be evaluated by hand. Numerical simulations showed that the dependency of the multiple access interference (MAI) toward the pulse shape reduces as the number of active users increases.

The crest factors of the DS-CDMA signals with different pulse shapes are compared with those of the MC-CDMA system. It is found that the crest factors of DS-CDMA signals are dependent solely on the pulse shaper, while the signals in MC-CDMA depends not only on the pulses, but also the signature sequences used. We also introduce a new type of sequences called spectrally efficient complementary (SEC) sequences, which can be used to constitute MC-CDMA signal waveforms that have a low crest factor and sharp roll-off gradient of the transmitted power spectrum; and they are found to be an alternative to the orthogonal sequences. The performance comparison of the DS-CDMA and MC-CDMA can be summarized in Table 5.1.

Comparison of crest factors		
Filter	**DS-CDMA** (*PN-seq.*)	**MC-CDMA** (*compl. seq.*)
Time-Limited	1 (0dB)	≤ 2 (6dB)
Ideally Band-Limited	$\approx \log N$ ($\approx 20 \log\log N$dB) where N = seq. length	≤ 2 (6dB)
Raised-Cosine	bounded, but $\uparrow$ as $r \downarrow$	≤ 2 (6dB)

Table 5.1: Summary of Crest factors.

Several general construction of SEC sequences are given and some fundamental properties of SEC sequences are derived. Up to now, SEC sequences were found to be limited by its length, and only sequences of length 2, 8 and 32 are found to be existed with length less than 40, which is consistent with the works of Golay [39] and Andres [40]. A generalized multiphase spectrally efficient complementary (MPSEC) sequences are derived from the SEC sequences and its construction methods are found to be nearly the same as that of SEC sequences with a slight modification. We successfully found MPSEC sequences of length 2, 4, 8, 10 and 16. It is expected that a lot of them can be found with a specified length so as to generate spectrally efficient low-crest waveforms for the future broadband MC-CDMA system.

5.2 Topics for Future Research

Performance Analysis using Improved Gaussian Approximation

It is noted that in chapter 3, we obtain the basic capacity formula of MC-CDMA by the standard Gaussian approximation. It is known that the performance can be evaluated using improved Gaussian approximation (I.G.A.) [41] to enhance the accuracy of the analysis. However, the complexities using I.G.A. in the calculation of MC-CDMA is far greater than those of the DS-CDMA. It may therefore worthwhile to do research on estimating the performance of the MC-CDMA in that fashion.

Effects of Turbo Codes on MC-CDMA

Turbo codes is a newly proposed coding technique in communication systems [42, 43]. It was claimed that with 2-PSK or 4-PSK, the system with turbo codes performs better than those with trellis-coded modulation (TCM) [43]. Turbo codes are constructed by concatenating two recursive systematic convolutional (RSC) codes with the decoder made of a P pipelined identical modules [44]. Recently, it has been used in the application of DS-CDMA [45], and it is interesting if we compare the performance with the Turbo-coded MC-CDMA system.

Guard-Time Analysis

In our analysis, we assumed that the signals in every tones (i.e. $f_0, 2f_0, 3f_0, \ldots$) of the MC-CDMA signal are synchronized with zero guard-interval ($f_0 = 1/T_s$). However, in burst-mode transmissions, one should not get rid of the guard-intervals. Analysis should be done for the system with different guard-intervals and obtain the system performance variations according to the change of: symbol-shapes; guard-intervals; and the number of carriers.

Crest Factor Analysis on Specific Sequences

In this thesis, we only focus on the crest factor analysis with the comparison between the subsequences of m-sequences on DS-CDMA with the Golay complementary sequenced MC-CDMA system. It may be desirable to do research on the crest factor performance issue with different PN sequence other than m-sequence (e.g. Gold, Kasami or Bent sequences) in DS-CDMA and compare with the MC-CDMA using Golay complementary sequences as signatures.

Appendix A

Exhaustive search of MPSEC sequences

In this section, $\{A, B\}$ is a pair of sequence for testing. We observed that the testing criterion would be (4.45) discussed earlier. However, we can use another criterion which save more computation time as the program runs for sequence searching.

Let us assume a, b, c, d and e, f, g, h be the frequencies of occurrence of '$+1$','-1','$+j$', and '$-j$' in A and B respectively, while the sequences A and B are of length N. Then, we can obtain the autocorrelation function of A as:

$$\begin{aligned} R_A(\tau) &= (a^2+b^2+c^2+d^2)(+1)+(ab+ba+cd+dc)(-1) \\ &\quad +(ca+ad+bc+db)(+j)+(ac+da+cb+bd)(-j) \end{aligned} \tag{A.1}$$

If we only count all the values of τ but $\tau = 0$, the autocorrelation function becomes

$$R_A(\tau, \tau \neq 0) = (a^2+b^2+c^2+d^2) - 2(ab+cd) - N. \tag{A.2}$$

Similarly, we have

$$R_B(\tau, \tau \neq 0) = (e^2+f^2+g^2+h^2) - 2(ef+gh) - N. \tag{A.3}$$

Using the complementary property (4.42), the summation (A.2) and (A.3) equals zero. Therefore, the testing condition for a pair of complementary sequences $\{A, B\}$ is:

$$(a-b)^2+(c-d)^2+(e-f)^2+(g-h)^2 = 2N. \tag{A.4}$$

Further if $A = \{\alpha_n\}$ is a MPSEC sequence which satisfies $\sum_{n=1}^{N}(-1)^n\alpha_n = 0$, then we have $a = b$ and $c = d$. Substitute in (A.4), we get a necessary but not sufficient condition to obtain a MPSEC sequence from a pair of testing sequences $\{A, B\}$:

$$(e - f)^2 + (g - h)^2 = 2N. \tag{A.5}$$

A flowchart of the testing scheme is shown in Figure A.1, where a numeric list is first stored before it is converted to a pointer of structure with both the *real* and *imaginary* parts. Then special functions and procedures are written to manipulate the complex additions and multiplications. Afterwards, autocorrelation of the two lists is then calculated and different *even-length* sequences are searched exhaustively.

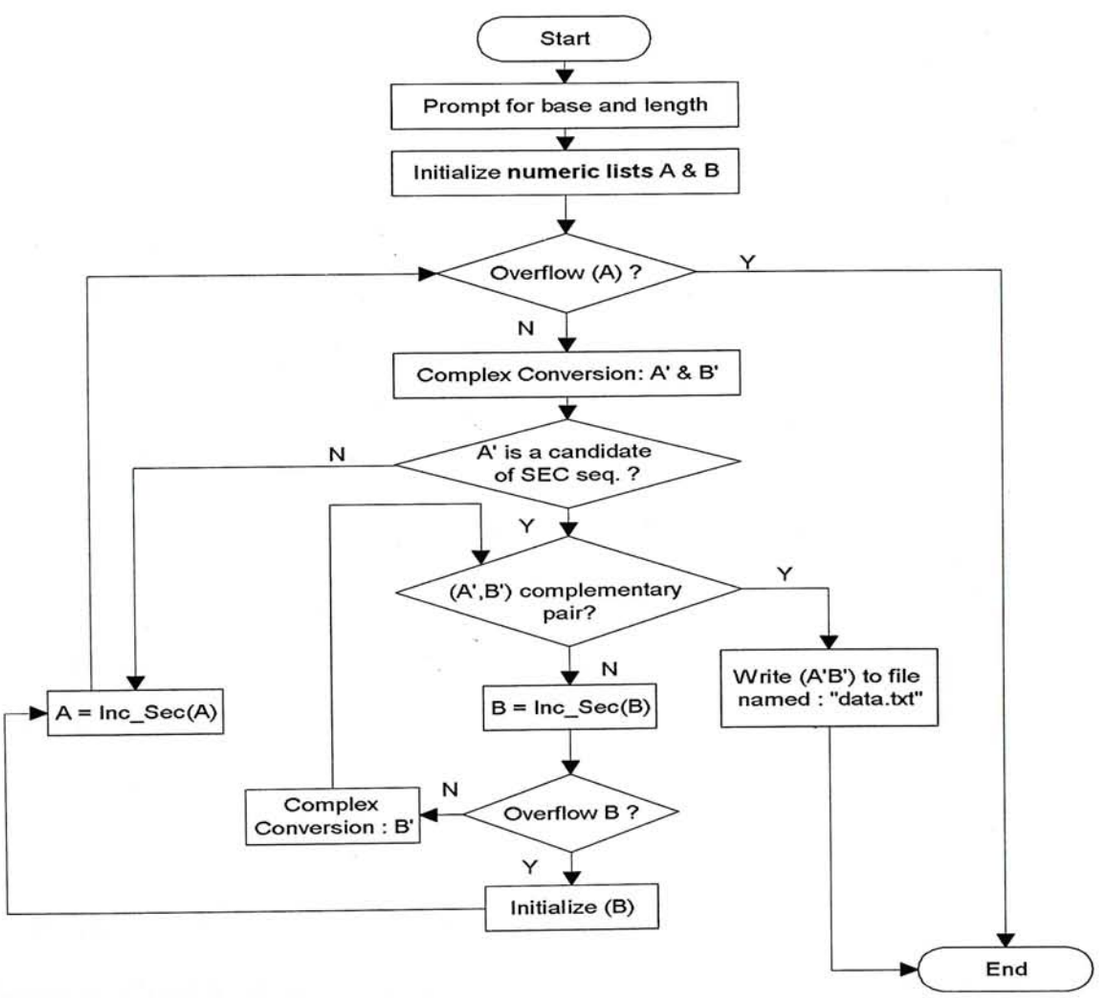

Figure A.1: Flowchart of the exhaustive search for MPSEC sequences.

Appendix B

Papers derived from this thesis

(1) T. F. Ho and Victor K. Wei, "On the Spectrally Efficient Low-Crest Waveforms Design of Multicarrier CDMA Systems," submitted to the *IEEE Transactions on Information Theory.*

(2) T. F. Ho, "Performance Evaluation for Multi-Carrier CDMA System," in *IEEE Vehicular Technology Conference Proc.*, pp. 1101-1105, May 1996.

(3) T. F. Ho and Victor K. Wei, "Construction of Spectrally Efficient Low-Crest Waveforms for Multicarrier CDMA Systems," in *International Conference on Universal Personal Communications Proc.*, pp. 522-526, November 1995.

(4) T. F. Ho and Victor K. Wei, "Synthesis of Low-Crest Waveforms for Multicarrier CDMA System," in *Communicatons Theory Mini-Conference in conjunction with IEEE Globecom Proc.*, pp. 131-135, November 1995.

(5) T. F. Ho, J. H. Yooh, C. K. Yeung, and Victor K. Wei, "Some Results on Multicarrier CDMA Wireless Communications," in *the 2d Workshop on Networking, Wireless, and Optical Technologies in Beijing*, July 4-6, 1995.

Bibliography

[1] R. L. Pickholtz, D. L. Schilling, and L. B. Milstein, "Theory of Spread-Spectrum Communications — A Tutorial," *IEEE Transactions on Communications*, vol. COM-30, pp. 885–884, May 1982.

[2] R. C. Dixon, *Spread Spectrum Systems.* John Wiley and Sons, 2nd edition ed., 1984.

[3] M. K. Simon, J. K. Omura, R. A. Scholtz, and B. K. Levitt, *Spread Spectrum Communications Vol. I-III.* Computer Science Press, 1985.

[4] S. Bible, *Spread Spectrum - It's not just for breakfast anymore!*, 1995. N7HPR, Reprinted from Digital Communications, column by Harold E. Price, NK6KQEX.

[5] T. S. D. Tsui and T. G. Clarkson, "Spread-Spectrum Communication Techniques," *Electronics and Communication Engineering Journal*, pp. 3–12, February 1994.

[6] G. Toole, "Emerging Technologies for Mobile Services Operating Above 1GHz," *Proceedings of Business and Technology Forum on Telecommunications (Hong Kong)*, pp. 1–9, September 1995.

[7] J. A. C. Bingham, "Multicarrier Modulation for Data Transmission : An Idea Whose Time Has Come," *IEEE Communications Magazine*, pp. 5–14, May 1990.

[8] T. M. Cover and J. A. Thomas, *Elements of Information Theory.* Wiley Series in Telecommunications, John Wiley and Sons, 2nd edition ed., 1991.

[9] J. M. Cioffi, "A Multicarrier Primer," Tech. Rep. T1E1.4/91-157, Amati Communications Corporation and Stanford University, November 1991.

[10] J. Leonard J. Cimini, "Analysis and simulation of a digital mobile channel using Orthogonal Frequency Division Multiplexing," *IEEE Transaction on Communications*, vol. COM-33, pp. 665–675, July 1985.

[11] J. G. Proakis, *Digital Communications.* Computer Science Series, McGraw Hill, International 2nd edition ed., 1989.

[12] S. H. Jamali and T. Le-Ngoc, *Coded-Modulation Techniques For Fading Channels.* The Kluwer Internatinal Series In Engineering and Computer Science, Kluwer Academic Publishers, 1994.

[13] P. M. Crespo, M. L. Honig, and J. A. Salehi, "Spread-Time Code-Division Multiple Access," *IEEE Transaction on Communications*, vol. COM-43, pp. 2139–2148, June 1995.

[14] Q. Chen, E. S. Sousa, and S. Pasupathy, "Performance of Coded Multi-Carrier DS-CDMA System in Multi-Path Fading Channels," 1995.

[15] K. Fazel, "Performance of CDMA/OFDM for mobile communication system," in *IEEE 2nd International Conference on Universal Personal Communications (ICUPC) Proc.*, October 1993.

[16] M. B. Pursley, "Performance Evaluation for Phase-Coded Spread-Spectrum Multiple-Access Communication – part I: System Analysis," *IEEE Transactions on Communications*, vol. COM-25, pp. 795–799, August 1977.

[17] A. W. Lam and S. Tantaratana, *Theory and Applications of Spread-Spectrum Systems.* IEEE Educational Activities Board Self-Study Course, May 1994.

[18] L. Vandendorpe, "Multitone Spread Spectrum Multiple Access Communications System in a Multipath Rician Fading Channel," *IEEE Transactions on Vehicular Technology*, vol. VT-44, pp. 327–337, May 1995.

[19] P. A. Bello, "Characterization of Randomly Time-Variant Linear Channels," *IEEE Transactions on Communication System*, vol. CS-11, pp. 360–393, December 1963.

[20] D. E. Borth and M. B. Pursley, "Analysis of Direct-Sequence Spread-Spectrum Multiple-Access Communication Over Rician Fading Channels," *IEEE Transactions on Communications*, vol. COM-27, pp. 1566–1577, October 1979.

[21] D. Parsons, *The Mobile Radio Propagation Channel.* Pentech Press, 1992.

[22] G. Santella, "Bit error rate performance of M-QAM Orthogonal Multicarrier modulation in presence of time-selective multipath fading," in *IEEE International Conference on Communications Proc.*, pp. 1683–1688, June 1995.

[23] F. G. Stremler, *Introduction to Communication Systems.* Addition Wesley, 3rd ed., 1990.

[24] Y. Asano, Y. Daido, and J. M. Holtzman, "Performance Evaluation for Bandlimited DS-CDMA Communications System," in *43rd IEEE Vehicular Technology Conference Proc.*, pp. 464–468, July 1993.

[25] R. Li and G. Stette, "Waveform Shaped MCM for Digital Microwave Radio," in *IEEE International Conference on Communications*, pp. 1695–1699, July 1995.

[26] S. U. Zaman and K. W. Yates, "Multitone Synchronization For Fading Channels," in *IEEE International Conference on Communications Proc.*, pp. 946–949, May 1994.

[27] G. Maral and M. Bousquet, *Satellte-Communications Systems : systems, techniques, and technology.* Chichester ; New York : Weley, 2nd ed., 1993.

[28] T. T. Ha, *Solid-State Power Amplifier Design.* Kriefer Publishing Company Malabar, Florida, reprint ed., 1991.

[29] K. J. Parsons, P. B. Kenington, and J. P. McGeehan, "Efficient Linearisation of RF Power Amplifiers For Wideband Applications," in *Proceedings of IEE*, pp. 7/1–7/7, 1994.

[30] S. Boyd, "Multitone Signals with Low Crest Factor," *IEEE Transactions on Circuits and Systems*, vol. CAS-33, pp. 1018–1022, October 1986.

[31] M. R. Schroeder, *Number Theory in Science and Communication : with applications in cryptography, physics, digital Information, computing and self-similarity.* Springer-Verlag, 1986.

[32] L. J. Greenstein and P. J. Fitzgerald, "Phasing Multitone Signals to Minimize Peak Factors," *IEEE Transactions on Communications*, vol. COM-29, pp. 1072–1074, July 1981.

[33] M. R. Schroeder, "Synthesis of Low-Peak-Factor Signals and Binary Sequences With Low Autocorrelation," *IEEE Transactions on Information Theory*, pp. 85–90, January 1970.

[34] B. M. Popović, "Synthesis of Power Efficient Multitone Signals with Flat Amplitude Spectrum," *IEEE Transactions on Communications*, vol. COM-39, pp. 1031–1033, July 1991.

[35] J. E. Golay, "Complementary Series," *IRE Transactions on Information Theory*, pp. 82–87, April 1961.

[36] R. L. Frank, "Polyphase Complmentary Codes," *IEEE Transactions on Information Theory*, vol. IT-26, pp. 641–647, November 1980.

[37] C. C. Tseng and C. L. Liu, "Complmentary Sets of Sequences," *IEEE Transactions on Information Theory*, vol. IT-18, pp. 644–652, September 1972.

[38] R. Sivaswamy, "Multiphase Complementary Codes," *IEEE Transcations on Information Theory*, vol. IT-24, pp. 546–552, September 1978.

[39] B. P. Schweitzer, *Generalized Complementary Code Sets.* PhD thesis, University of California – Los Angeles, 1972.

[40] T. H. Andres, "Some Combinational Properties of Complementary Sequences," Master's thesis, The University of Manitoba, 1977.

[41] J. M. Holtzman, "Multitone Signals with Low Crest Factor," *IEEE Transactions on Circuits and Systems*, vol. CAS-33, pp. 1018–1022, October 1986.

[42] O. Joerssen and H. Meyr, "Terminiating the Trellis of Turbo-Codes," *Electronics Letters*, vol. 30, pp. 1285–1286, August 1994.

[43] S. L. Goff, A. Glavieux, and C. Berrou, "Turbo-Codes and High Spectral Efficency Modulation," in *IEEE International Conference on Communications*, pp. 645–649, 1994.

[44] C. Berrou, A. Glavieux, and P. Thitimajshima, "Near Shannon Limit Error - Correcting Coding and Decoding : Turbo-Codes (1)," in *43th IEEE Vehicular Technology Conference*, pp. 1604–1070, 1993.

[45] P. Jung, M. NaBhan, and J. Blanz, "Application of Turbo-Codes to a CDMA Mobile Radio System Using Joint Dectection and Antenna Diversity," in *44th IEEE Vehicular Technology Conference*, pp. 770–774, 1994.

CUHK Libraries
003511117